creative commons
COMMONS DEED

저작자표시-비영리-변경금지 2.0 대한민국

이용자는 아래의 조건을 따르는 경우에 한하여 자유롭게

- 이 저작물을 복제, 배포, 전송, 전시, 공연 및 방송할 수 있습니다.

다음과 같은 조건을 따라야 합니다:

저작자표시. 귀하는 원저작자를 표시하여야 합니다.

비영리. 귀하는 이 저작물을 영리 목적으로 이용할 수 없습니다.

변경금지. 귀하는 이 저작물을 개작, 변형 또는 가공할 수 없습니다.

- 귀하는, 이 저작물의 재이용이나 배포의 경우, 이 저작물에 적용된 이용허락조건을 명확하게 나타내어야 합니다.
- 저작권자로부터 별도의 허가를 받으면 이러한 조건들은 적용되지 않습니다.

저작권법에 따른 이용자의 권리는 위의 내용에 의하여 영향을 받지 않습니다.

이것은 이용허락규약(Legal Code)을 이해하기 쉽게 요약한 것입니다.

Disclaimer

dCollection

理學博士學位論文

Non-canonical regulation of Fructose metabolism by FruR in *Vibrio cholerae*

비브리오 콜레라균 FruR에 의한 비 전형적 방식의 과당대사조절

2020년 2월

서울大學校 大學院

生命科學部

尹 昌 奎

Non-canonical regulation of Fructose metabolism by FruR in *Vibrio cholerae*

by

Chang-Kyu Yoon

Under the supervision of

Professor Yeong-Jae Seok, Ph. D

A Thesis for the Degree of **Doctor of Philosophy**

February, 2020

School of Biological Sciences

Seoul National University

비브리오 콜레라균 FruR에 의한
비 전형적 방식의 과당대사조절

指導敎授 石 暎 宰

이 論文을 理學博士 學位論文으로 提出함
2019年 12月

서울大學校 大學院
生命科學部
尹 昌 奎

尹昌奎의 理學博士學位論文을 認准함
2019年 12月

委 員 長 _____

副委員長 _____

委 員 _____

委 員 _____

委 員 _____

ABSTRACT

Non-canonical regulation of fructose metabolism by FruR in *Vibrio cholerae*

Chang-Kyu Yoon
School of Biological Sciences
The Graduate School
Seoul National University

In most bacterial species, fructose uptake is mediated by the fructose-specific phosphoenolpyruvate (PEP)-dependent carbohydrate phosphotransferase (PTS^{Fru}). The PTS^{Fru} consists of FruA, membrane-spanning protein that is responsible for fructose transport, and FruB that delivers a phosphate group from PEP to FruA, which finally phosphorylates the fructose during its transportation across the membrane. While most PTS sugars are phosphorylated at their 6-position, fructose is phosphorylated at 1-position. Fructose 1-phosphate (F1P) is then converted to fructose 1,6-bisphosphate (FBP) by 1-phosphofructokinase (FruK). In bacteria belonging to *Gammaproteobacteria* including *Escherichia coli*, *Pseudomonas putida* and *Vibrio cholerae*, FruA, FruB and FruK are encoded in a single operon (*fruBKA*). It has been known that, in most bacteria possessing the *fruBKA* operon such as *E. coli* and *P. putida*, transcription of the *fruBKA* operon is negatively regulated by the fructose repressor (FruR) which binds to the cognate operator(s) located downstream of the transcription start site (TSS) of the operon and F1P is the inducer of this operon. However, this study reveals that the FruR-mediated

transcriptional regulation of the *fruBKA* operon in *V. cholerae* is completely different and more sophisticated than that of *E. coli* and *P. putida*. In *V. cholerae,* FruR is essential for the transcription of the *fruBKA* operon and the growth on fructose. FruR directly binds to three cognate operators located at the intergenic region between the gene coding for FruR itself and the *fruBKA* operon. Among these operators, the operator centered at 20.5 bp upstream of the TSS of the *fruBKA* operon is essential but the other two operators are dispensable for the activation of the *fruBKA* transcription and thus the growth of *V. cholerae* on fructose. Furthermore, the FruR-mediated transcriptional activation requires an intracellular F1P. The exogenous expression of FruR mutants defective in F1P recognition could not complement the growth defect of a *fruR* mutant on fructose. The binding properties of the FruR to the operators are altered by F1P so that FruR enables the RNA polymerase to activate the transcription of the *fruBKA* operon. Taken together, in this study shows the non-canonical regulation of the *fruBKA* expression by FruR in *V. cholerae*.

Key words:

Fructose metabolism; PTS^{Fru}; FruR; F1P; Transcriptional regulation; *V. cholerae*

***Student Number*: 2013-20310**

Contents

List of Figures

List of Tables

ABBREVIATIONS

6-FAM; 6-Carboxyfluorescein

Arg; Arginine

Asn; Aspargin

cAMP; cyclic-AMP

Cra; Catabolite repressor/activator

CRP; cAMP receptor protein

DTT; dithiothreitol

E_co; *E. coli*

EcCore*; E. coli* RNA polymerase Core enzyme

EDTA; ethylenediaminetetraacetic acid

EMSA; electrophoretic mobility shift assay

F1P; fructose 1-phosphate

F6P; fructose 6-phosphate

FBP; fructose 1, 6-bisphosphate

Fru; fructose

G6P; glucose-6-phosphate

GalR; galactose repressor

Glc; glucose

HEX; Hexachloro-fluorescein

HTH motif; Helix-turn-Helix motif

IPTG; isopropyl-β-D-1-thiogalactopyranoside

LacI; lactose inhibitor (repressor)

***N*-AcGlcN; N-acetylglucosamine**

***N*-AcMur; N-acetylmuramic acid**

ONPG; o-nitrophenyl-β-D-galactopyranoside

P_pu; *P. putida*

PEP; Phosphoenolpyruvate

PTS, phosphoenolpyruvate: carbohydrate phosphotransferase system

Pyr; Pyruvate

SDS; sodium dodecyl sulfate

TF; Transcription factor

TSS; transcription start site

V_ch; *V. choleare*

Vcσ70; *V. cholerae* Sigma factor 70

X-gal; 5-bromo-4-chloro-3-indolyl-β-D-galactopyranoside

Chapter I. Introduction

1. Sugar-mediated signal transduction systems in bacteria

1.1. Phosphoenolpyruvate (PEP): carbohydrate phosphotransferase system (PTS)

Group translocation of carbohydrates is mediated by the bacterial phosphoenolpyruvate (PEP): carbohydrate phosphotransferase system (PTS) which uses PEP to phosphorylate a number of hexoses including *N*-acetylmannosamine, glucose, mannose, glucosamine, and *N*-acetylglucosamine (Kundig *et al.*, 1964). The PTS catalyzes the uptake of with a concomitant phosphorylation of numerous carbohydrates and regulates many metabolic functions of the cell including transport of particular sugars. It is composed of two general cytoplasmic proteins, enzyme I (EI) and the histidine-containing phosphocarrier protein (HPr), which are commonly used to transport many PTS sugars, and various sugar-specific enzyme II (EII) complexes (Barabote & Saier, 2005). Each EII complex usually consists of two cytoplasmic domains, EIIA and EIIB, and one transmembrane domain, EIIC. The number and structure of the EII complexes vary between species while the amino acid sequences of EI and HPr are strongly conserved in all bacteria. EI and HPr mediate phosphoryl transfer from PEP to EII, which leads to the phosphorylation of a PTS sugar during its transport into the cell. Specifically, EI, HPr and EIIA are phosphorylated at histidine and EIIB domains are phosphorylated at either cysteine or histidine depending on the particular transporter (Siebold *et al.*, 2001).

1.2. One-component system

Bacteria possess simplified transduction machinery termed the one component system (Ulrich *et al.*, 2005). One component system refers to a sensory transcriptional factor that has both input and output domain. This system has diverse input domains such as PAS (found in period clock protein,

aryl hydrocarbon receptor, and single-minded protein), GAF (found in mammalian cGMP-binding phoshodiesterases, Anabaena adenylyl cyclases, and *E. coli* FhlA) and various small molecule-binding domains and output domains whose activity is regulation of gene espression at the level of transcription. Most of well-known small-molecule-dependent repressors or activators that regulate the transcription of prokaryotic operons such as lactose repressor (LacI) and cyclic-AMP (cAMP) receptor protein (CRP) are members of this system. Since a transcription factor directly senses the intracellular level of a metabolite, it is considered as the most primitive, simple and effective signal transduction system in bacteria.

1.3. Fructose derivates as metabolite effectors

When minimal medium was supplemented with 26 different nutrients, the expression pattern of about one hundred genes related to the central carbon metabolism changed in *E. coli* (Kochanowski *et al.*, 2017). It was reported that 70% of these changes are caused by general transcriptional regulation, which is dependent on the growth of the bacterium. The rest 20% could be explained by the specific transcription factor sensing the intracellular level of specific metabolites such as cAMP, fructose 1,6-bisphosphate (FBP) and fructose 1-phosphate (F1P). Unlike the nucleotide-based molecule cAMP, the FBP and F1P are the intermediates derived from the metabolism of fructose.

2. Fructose metabolism in *Vibrio cholerae*

2.1. The importance of the fructose metabolism

There are several evidences suggesting that fructose may have been important in the early evolution of carbohydrate metabolic pathways in bacteria. First, fructose is the only sugar that feeds directly into the Embden-Meyerhof glycolytic pathway without isomerization or epimerization (Saier & Ramseier,

1996). Second, some bacterial genera possess the high-affinity fructose-specific PTS, but they apparently cannot phosphorylate other sugars via the PTS (Gupta & Ghosh, 1984, Lessie & Phibbs, 1984). Third, fructose is one of the few sugars that can be utilized efficiently even in the absence of cAMP or CRP (Feldheim *et al.*, 1990).

2.2. Overview of the fructose metabolism

2.2.1. Fructose transport via the PTS

The metabolism of fructose initiates from the transport through the fructose-specific PTS (PTS^{Fru}). The system consists of the cytosolic fructose-specific $EIIA^{Fru}$-FPr proteins and membrane-spanning EIIBB'C (Kornberg, 2001). When fructose is translocated into the cell through EIIBB'C (encoded by *fruA*), $EIIA^{Fru}$-FPr (encoded by *fruB*) transfers a phosphoryl group from EI to EIIBB'C, which converts the transported fructose into F1P. The fructose PTS is unique in that it possesses its own HPr-like protein domain, FPr, which is fused to the EIIA domain in the *fruB* gene.

In *E. coli*, It is known that fructose also transported through alternative PTSs that have a general ability to recognize sugars possessing the 3,4,5-D-arabino-hexose configuration including the PTSs for mannose, mannitol and glucitol (Ferenci & Kornberg, 1974, Yamada & Saier, 1987, Grisafi *et al.*, 1989). Furthermore, *E. coli* has three silent gene clusters (*frv, frw, frx*) that uniquely encodes silent backup fructose PTSs with unknown physiological function (Reizer *et al.*, 1995). It is known that fructose translocated through these transporters is modified into fructose-6-phosphate (F6P).

2.2.2 1-phosphofructokinase (FruK)

F1P is converted into FBP by ATP and 1-phosphofructokinase (FruK). The gene coding for FruK is in the middle of operon encoding the PTS^{Fru}. FruK

exhibits little sequence identity with 6-phosphofuctokinase which converts the F6P into FBP which is encoded in *pfkA* and *pfkB* of *E. coli* (Kornberg, 2001). A recent study reported that FruK can exhibit the reverse enzymatic activity resulting in generation of F1P from FBP in specific circumstances (Singh *et al.*, 2017)

2.3. Fructose metabolic genes in *Vibrio* species

2.3.1 Genetic redundancy of the fructose PTS in *V. cholerae*

In *V. cholerae*, there are 25 homologs of PTS components responsible for transporting 10 types of carbohydrates. The carbohydrate specificities of each PTS component have been defined (Figure 1) (Houot & Watnick, 2008, Houot *et al.*, 2010a, Houot *et al.*, 2010b, Hayes *et al.*, 2017). There are redundant genes encoding PTS components specific for fructose among the 10 types of sugar-specific PTS genes in the *V. cholerae* genome. The major fructose-specific PTS is comprised of the membrane-spanning transporter FruA (locus name: VCA0516) and cytosolic FruB (locus name: VCA0518). Other putative fructose-specific PTS components were also identified (VC1820-24) while their specific substrates were not determined except for VC1820-21, which suggested as the facilitated glucose transporter, FdgA (Hayes *et al.*, 2017).

2.3.2 Transcriptome analysis of fructose metabolic genes in *Vibrio* species

A previous work examined whether transcription of major PTS component gene was modulated by the availability of a specific substrate. Among the fructose PTS genes, the transcription of *fruB* increased approximately 80-fold in minimal medium containing fructose, in contrast to the minimal medium containing no sugar (Houot *et al.*, 2010a). However, the mechanism of induction was not thoroughly investigated.

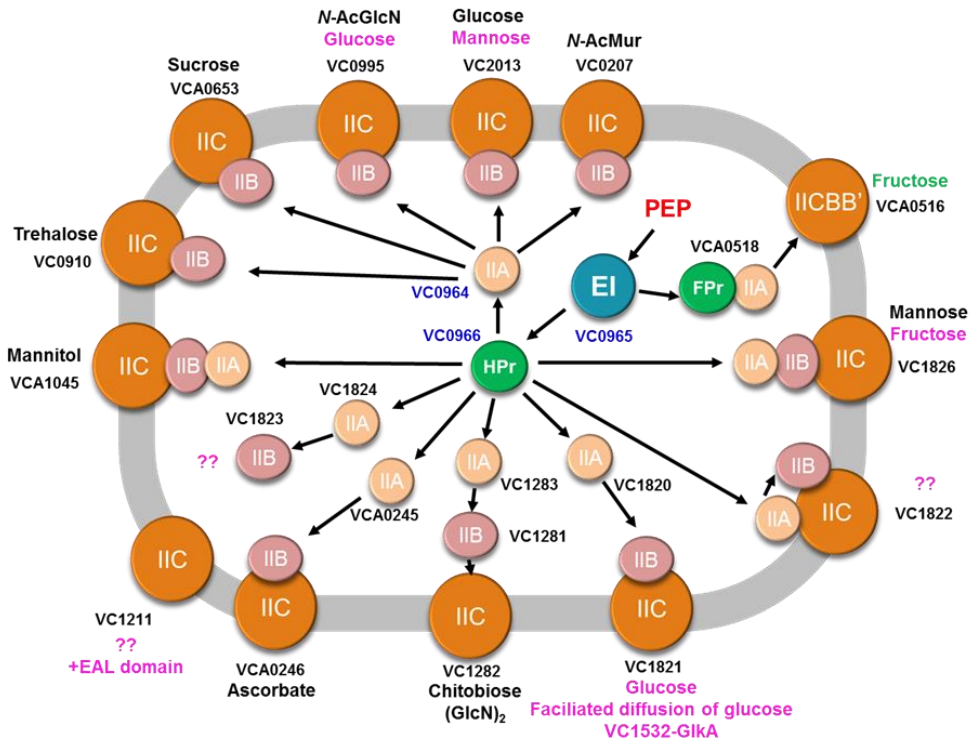

Figure 1. The schematics of PTS components in *V. cholerae*

The PTS consists of two general components, Enzyme I and HPr and the sugar specific components Enzymes II A-C. The primary role of these components is to catalyze phosphorylation coupled to translocation of sugars across the cytoplasmic membrane. PTS components also participate in other physiological mechanisms through the direct protein-protein interaction with other proteins. The *V. cholerae* genome encodes 25 PTS components, including two of EI homologs, three of HPr homologs, and nine of EIIA homologs (10 sugars). *N*-AcGlcN; N-acetylglucosamine, *N*-AcMur; N-acetylmuramic acid.

Many experimental evidences show that the PTS genes including fructose-specific ones are up-regulated during host infection in *Vibrio* species (Table 1) (Mandlik *et al.*, 2011, Livny *et al.*, 2014, Jang *et al.*, 2017). Thus, it is necessary to integrate experimental data to define the direct link between the transcriptional regulation and the utilization of external fructose.

3. Transcriptional regulation by Fructose repressor (FruR)

3.1 Overview of LacI/GalR family transcription factors

FruR belongs to the LacI/GalR type of transcriptional regulators. This type of transcription factors(TFs) have a conserved DNA binding domain at their N-terimini and a metabolite effector-binding domain (Weickert & Adhya, 1992). These TFs bind to operator(s) as a dimer or tetramer and concomitantly induces DNA looping or bending (Swint-Kruse & Matthews, 2009). LacI/GalR type of TFs bind to tandem operators, which enables the cooperative binding of transcription factors for tight regulation of the target genes (Ravcheev *et al.*, 2014). For example, LacI binds to three operators in the promoter region of the *lacZYA* operon (Oehler *et al.*, 1990) and PurR binds to two operators of the gene encoding itself to autoregulate its expression (Rolfes & Zalkin, 1990).

3.2. Molecular mechanism of FruR-mediated transcriptional regulation

3.2.1 DNA binding properties of FruR

In *E. coli*, FruR (EcFruR) binds to the two operators O1 (GC- TGAAAC/ GTTTCA-AG) and O2 (GC-TGAATC/GTTTCA-AT), centered at 7.5bp and 73.5bp downstream of the transcription start site (TSS) of *fruBKA*, respectively (Shimada *et al.*, 2011). In the absence of a metabolite effector, the EcFruR binding to the promoter region of *fruBKA* operon leads to a physical hindrance for RNA polymerase to access the promoter, resulting in

Table 1. The literature review of transcriptional regulations of PTS genes in *Vibrio* species

Vibrio parahaemolyticus

locus tag	gene product	fold change
VP0794	phosphoenolpyruvate-protein_phosphotransferase (EI)	6.02
VP0795	HPr	3.25
VPA0297	**fructose-specific IIBC component**	34
VPA0298	**fructose-specific IIA component**	21
VP0795	**HPr**	3.25
VPA1424	**fructose-specific IIABC component**	5.5
VPA1429	hypothetical protein	12.9

V. cholerae

locus tag	gene product	fold change
VC0910	Trehalose-specific IIBC component	0.03
VC1283	cellobios-specific IIA component	0.24
VC1820	**fructose-specific IIA component**	**0.32**
VCA0516	**fructose-specific IIBC component**	**26.98**
VCA0518	**fructose-specific IIA/FPr component**	**68.36**
VCA0245	ascorbate-specific IIA component	154.33
VCA0246	ascorbate-specifict IIC/B componen	54.11
VCA0519	**fructose repressor**	**15.09**

Vibrio vulnificus

locus tag	gene product	fold change
VVMO6_02633	mannitol-specific IIABC component	5.92
VVMO6_03150	**fructose-specific IIABC component**	**176.2**
VVMO6_03154	**fructose-specific IIABC component**	**4.11**
VVMO6_03157	**fructose-specific IIBC component**	**45.90**
VVMO6_04473	ascorbate-specific PTS system EIIA component	11.81
VVMO6_04531	*N*-acetylmuramic acid-specific IIBC component	11.23

transcriptional repression of the *fruBKA* operon. A homo-tetramer of EcFruR induces the DNA looping (Cortay *et al.*, 1994).

3.2.2 Metabolite effector of FruR

Direct binding of a metabolite effector modulates the DNA binding affinity of FruR. It has been widely accepted that FruR can bind to a phosphorylated fructose. It was previously shown that FBP at a milli-molar level and F1P at a micro-molar level affect the activity of EcFruR (Ramseier *et al.*, 1995). However, recent studies represented convincing evidences that at a physiological concentration range, F1P but not FBP is the metabolite effector of EcFruR (Bley Folly *et al.*, 2018). Authors suggest that the effect of a milli-molar concentration of FBP on the *in vitro* EcFruR activity is because of the contamination of F1P in the commercial FBP. Furthermore, the well-known FruR ortholog in *Pseudomonas putida* (PpFruR) also binds only to F1P yet not FBP in regulating the expression of the *fruBKA* operon (Chavarria *et al.*, 2011, Chavarria *et al.*, 2014).

3.3. Catabolite repressor/activator (Cra) as a global regulator

3.3.1 Global transcriptional regulation of Cra

As EcFruR was revealed to be involved in the regulation of other genes related to overall metabolic pathways including glycolysis, TCA cycle and gluconeogenesis, FruR was renamed as Catabolite Repressor Activator (Cra) (Ramseier *et al.*, 1993, Ramseier *et al.*, 1995). Many previous studies have examined to identify the underlying molecular mechanism of FruR on the regulation of diverse metabolic genes (Cortay *et al.*, 1994, Ryu *et al.*, 1995, Bledig *et al.*, 1996, Mikulskis *et al.*, 1997, Crasnier-Mednansky *et al.*, 1997, Negre *et al.*, 1998, Prost *et al.*, 1999). Later, FruR was regarded as a global transcriptional regulator linking the metabolic flux signal, the intracellular

concentration of FBP, to the regulation of mRNA expression levels of metabolic genes. FruR seems to control the genes encoding enzymes of the central carbon metabolism through binding to almost 160 sites in the *E. coli* genome (Shimada *et al.*, 2005, Sarkar *et al.*, 2008, Shimada *et al.*, 2011). Furthermore, recent studies have shown that EcFruR not only directs the central carbon pathways but also forms an integrated metabolic network together with another major global regulator, cAMP receptor protein (CRP) (Kim *et al.*, 2018).

3.3.2 Molecular mechanism of global transcriptional regulation by Cra

A number of experimental evidence have compared the transcriptome of a *fruR* mutant with that of wild type (WT). These results showed that up to 50 genes were differentially expressed depending on the presence of FruR (Sarkar *et al.*, 2008), and the expression of 97 genes was altered by FruR binding (Kim *et al.*, 2018). The general rules to differentiate the repressor-FruR binding sites and activator-FruR binding sites are the distance and orientation of the binding sites relative to the TSS (Saier & Ramseier, 1996, Shimada *et al.*, 2011) and the binding affinity (K_d value) of FruR to DNA (Shimada *et al.*, 2005). EcFruR has been found to directly bind to the 14-bp-long FruR box with imperfect palindromic sequence (5'-GCTGAAnC/GnTTCA-3') (Shimada *et al.*, 2011)

3.4. FruR in diverse *Gammaproteobacteria*

A comparative genetic analysis revealed that the regulon size and the functioning mechanism of FruR correlates with the taxonomy of the studied group and with the phylogeny of the FruR proteins in *Gammaproteobacteria* (Ravcheev *et al.*, 2014). It is known that FruR of bacteria in *Vibrionales* and *Pseudomonadales* acts as a local transcription factor in contrast to the order

Enterobacteriales.

4. The aims of this study

Most of bacteria have preserved an efficient sugar transport system, PTS, and subsequent transcriptional regulation mechanisms in their genomes which enable the efficient utilization of this nutrient. F1P, a fructose metabolite produced by the PTS, regulates the expression of PTS components and metabolic genes along with the sensory transcriptional regulator, FruR. Molecular mechanism of the FruR-mediated transcriptional regulation has been investigated in *E. coli* and *P. putida*. In recent studies, it was reported that *Vibrio* species, which have genomic redundancy of fructose-specific PTSs, exhibit the significantly increased expression of fructose-specific PTS components during host infection. This study aims to validate the canonical mechanism of FruR-mediated transcriptional regulation and to investigate the transcriptional regulation according to nutrient environment in the host infection of *Vibrio* species by studying the transcriptional regulation mechanism of FruR in *V. cholerae*.

Chapter II. Material and Method

1. Bacterial strains, plasmids and culture conditions

All *V. cholerae* strains were cultured in Luria-Bertani (LB) medium or M9 minimal medium supplemented with indicated sugars at 37˚C. All *E. coli* strains were grown in LB medium at 37˚C. All plasmids were constructed using standard PCR-based cloning procedures and verified by sequencing. In-frame deletion mutants of *V. cholerae* were generated by allelic exchange using pDM4-based plasmid as described previously (Park *et al.*, 2019). We constructed pDM4-BR for chromosomal integration to generate the various *fruBR* mutants. 1 kb DNA fragments containing 338-bp of *fruR-fruBKA* intergenic region and 662-bp downstream region respect to the start codon of *fruB* or *fruR* were amplified by PCR and cloned into the corresponding site of pDM4. To introduce a mutation in the *fruR-fruBKA* intergenic region, site-directed mutagenesis PCR was performed. PCR with respective primers mutated the indicated operator into different 16-bp sequences with similar G/C, A/T ratio to *fruR* operator in the intergenic sequence. The *E. coli* SM10 λpir strain carrying various pDM4-based plasmids were conjugated with *V. cholerae* O1 El Tor N16961 and all transconjugants were confirmed by PCR as previously described (Kim *et al.*, 2015).

The plasmids except for pDM4-based plasmids were transformed into indicated *V.cholerae* strains using electroporation as previously described (Hamashima *et al.*, 1995). *V. cholerae* was grown in BHI (Brain Heart Infusion, BD) medium until OD_{600} reached 0.5. Cells were harvested and washed two times with 20-ml of ice-cold electroporation buffer (1 mM HEPES-NaOH pH 8.0, 137 mM sucrose). Cell pellets were resuspended with 50-ul of wash buffer. A 200 ng of plasmids were mixed with competent cells. After transferring the mixture to ice-chilled cuvette, samples were pulsed with a time constant of 6.1 ms at 2.48 kV (Bio-Rad).

To construct the VcFruR overexpressing plasmid, ORF of VcFruR was

amplified by PCR and cloned into appropriate site in pET43.1a vector. The following supplements were added if necessary: ampicillin, 100 μg ml $^{-1}$; chloramphenicol, 2 μg ml $^{-1}$; tetracyclin, 1 μg ml $^{-1}$for *V. cholerae* and ampicillin, 100 μg ml $^{-1}$; chloramphenicol, 10 μg ml $^{-1}$; tetracyclin, 20 μg ml $^{-1}$ for *E. coli*; isopropyl-β-D-1-thiogalactopyranoside (IPTG), 1 mM; 5-bromo-4-chloro-3-indolyl-β-D-galactopyranoside (X-gal), 80 μg ml $^{-1}$.

2. Determination of the growth curves of bacterial cells cultured in M9 medium supplemented with fructose or glucose

Overnight grown *V. cholerae* cultures were diluted 100-fold into fresh LB medium and cultured at 37˚C until OD_{600} reached 1.0. To minimize the unknown effect of sugar attributed from being cultured in complex medium, the cell pellets were washed two times with M9 medium without any carbon sources followed by cultures at the same medium for 30 min. Each strain was then inoculated into a 96-well plate (SPL) containing M9 medium supplemented with 0.2% of glucose or fructose and optical density of all cultures was measured at 600nm using a multimode microplate reader (TECAN Spark TM 10 M multimode microplate reader, Männedorf, Switzerland).

3. RNA extraction and Quantitative Real time PCR (qRT-PCR)

RNA extraction and qRT-PCR was done as previously described with modification (Park *et al.*, 2019). The indicated *V. cholerae* strains were grown at LB medium and washed with M9 medium in a same preparation manner as mentioned above. Each culture was divided into two identical samples, with one supplemented with 0.2% fructose and the other with 0.2% glucose. Each set of samples were cultured at 37˚C for 30 min. After fixing the cells with same volume of ice-chilled 100% methanol, total RNA was isolated using

MiniBEST Universal RNA Extraction Kit (Takara Bio). The 2500 ng of RNA from each sample was converted into cDNA using the EcoDryTM Premix (Takara Bio). The 30-fold diluted cDNA was subjected to real-time PCR amplification using FAST CYBR green master mix kit (Life Technologies) with specific primers in CFX96 Real-Time System (Bio-Rad). To normalize the transcript level, 16S rRNA (*rrsG*) was measured and used as a reference.

4. Eletrophoretic mobility shift assay (EMSA)

Non-radioisotope labeled EMSA was performed as previously described (Chavarria *et al.*, 2011). 338-bp DNA fragment covering the entire wild-type *fruR-fruBKA* intergenic sequence or fragments containing at least one mutated sequence were used as a probe. 40 ng or 60 ng of probes were incubated with indicated amount of purified proteins and metabolites in buffer containing 10 mM Tris-HCl (pH 8.0), 5 % v/v Glycerol, 0.1 mM ethylenediaminetetraacetic acid, EDTA, 1 mM dithiothreitol, DTT. Each sample was incubated at 37˚C for 10 min and then analyzed by 6% TBE (89 mM Tris, 89 mM Boric acid, 20 mM EDTA) based Native PAGE followed by EtBr staining. DNA bands were visualized in gel documentation system (Korea BioTech). To investigate whether the binding of the VcFruR protein affects DNA topology at each *fruR* operator, we constructed 215-bp probes which contain one each operator sequenc and two other mutated sequences using PCR. Bending angles were determined using the method described by previous study (Papapanagiotou *et al.*, 2007). Briefly, a distance between 5' end of the fragment and centre of the binding site was normalized to the full length of probe DNA and it is called as flexure displacement. The respective mobilities of FruR bound DNA complex (R_b) and the free probe (R_f) were calculated for all the probe. R_b values normalized to the respective R_f values (R_b/R_f), denoted as "y" were plotted against the flexure displacement value ,

denoted as “x”. The resulting plot was fitted to a quadratic equation: $y = ax^2 - bx + c$. Bending angle α is given by $a = -b = 2c(1-\cos\alpha)$. Quantification of the band intensity was achieved using ImageJ (http://rsb.info.nih.gov/ij/, NIH) program.

5. DNase1 footprinting

DNase1 footprinting experiments using 6-Carboxyfluorescein (6-FAM) labeled probe were done as demonstrated in the previous work (Choi *et al.*, 2017). A 320-bp 6-FAM labeled probe was generated by PCR with 6-FAM-labeled primers. To identify the footprints of RNA polymerase and/or Sigma factor (σ70), we constructed 538-bp 6-FAM labeled probe covering the sequence ranges from 100-bp downstream of the start codon of *fruB* to 100-bp downstream of the start codon of *fruR* using PCR. The purified PCR product was incubated with indicated amount of purified proteins or metabolites at 37˚C for 10 min prior to digestion with 0.02 units of DNase I (NEB) for 1 min. The cleavage reaction was stopped by adding the same volume of stop solution (200 mM NaCl, 30 mM EDTA, 1% sodium dodecyl sulfate, SDS) followed by phenol extraction and EtOH precipitation. Fragment sizes were determined in comparison to internal molecular weight standards. The DNase I digestion electropherograms were aligned with the manually generated sequence using the GeneMapper software (Applied Biosystem).

6. β-galactosidase assay

To construct the transcriptional *lacZ*-fusion plasmid, 338-bp of *fruR-fruBKA* intergenic region was amplified by PCR. The PCR product was digested with salI (NEB) and inserted into the corresponding site of promoter-less *lacZ* fusioned pJK1113 (pJK-Z), resulting in pJK1113-P_{fruB}-*lacZ* (pJK-BZ). Each

fruB operator were replaced into mutated sequence using the same PCR-based method to construct pDM4-*fruBR*.

The Δ*lacZ* or Δ*lacZ*Δ*fruR* strains harboring various pJK-BZ based constructs were treated with 0.2% glucose or fructose similar to the growth test except for incubating the samples 1 hr in sugar containing minimal medium. The cultured cell were lysed to measure the β-galactosidase activities of the cellular extracts as previously described (Lee *et al.*, 2018). A 80 μl of samples were 1/10 diluted with Z-buffer (0.06 M Na_2HPO_4, 0.04 M NaH_2PO_4, 0.01 M KCl, 1 mM $MgSO_4$, 0.04 M β-mercaptoethanol) followed by addition of 20 μl of 0.01% SDS and 40 μl of chloroform. After intense vortexing for 20 s, samples were incubated at 37˚C for 10 min for cell lysis. To this mixture, 160 μl of 4 mg ml^{-1} o-nitrophenyl-β-D-galactopyranoside (ONPG) was added and left at 25˚C for 5 min. Then, the reaction was stopped with 400 μl of 1 M $NaCO_3$ and the resulting yellow color was measured at 420 nm.

7. Purification of overexpressed proteins

The non-tagged VcFruR proteins and mutant forms of VcFruR proteins were overexpressed in *E. coli* BL21 (DE3)/pLysSRARE (Novagen). Harvested cells were resuspended in buffer A (50 mM Tris-HCl pH8.0, 50 mM NaCl, 10 mM DTT, 10 mM EDTA and 10% glycerol) and disrupted by three passage through a French pressure cell at 9,000 psi. After centrifugation at 100,000 × g at 4˚C for 60 min, the supernatant was subjected to a HiTrap Heparin HP affinity columns (GE Healthcare Life Sciences). The protein elution was performed using a 20-column volume gradient of 0.5–1 M NaCl in buffer B (50 mM Tris-HCl pH 8.0, 1 M NaCl, 10 mM DTT, 10 mM EDTA and 10% glycerol) at a flow rate of 2 ml min^{-1}. The fractions containing the VcFruR were concentrated, and then chromatographed on a HiLoad16/60

Superdex 200 pg column (GE Healthcare Life Sciences) equilibrated with buffer C (50 mM Tris-HCl, pH 8.0, 200 mM NaCl, 10 mM DTT, 10 mM EDTA and 10% glycerol) to achieve higher purity (>95%).

His-tagged proteins were overexpressed in *E. coli* ER2566 and purified using TALON metal-affinity resin (Takara Bio) according to the manufacturer's instructions. Proteins bound to resin were washed with buffer containing10 mM imidazole and eluted with buffer containing 200 mM imidazole. Eluted sample was further chromatogramed on a HiLoad 16/600 Superdex 200 pg column.

8. Determination of Oligomeric state of FruR

1 mg of VcFruR was injected into Superdex 200 10/300GL column and absorbance of eluted sample was measured at 280nm. Nine molecular weight markers (Black line) were used to calibrate column. Thyroglobulin (669 kDa); Apoferritin (443 kDa); β-amylase (200 kDa); Alcohol dehydrogenase (150 kDa); Albumin (66 kDa); Carbonic anhydrase (29 kDa); Cytochrome C (12.5 kDa); Aprotinin (6.5 kDa) (Sigma Aldrich). The molecular mass was plotted versus the V_e/V_0 value, where V_e, is the elution volume and V_0, is the void volume, as determined from the elution of blue dextran.

9. Primer extension

Primer extension analyses were carried out as previously described (Ryu *et al.*, 2012). *V. cholerae* total RNA was extracted from the cells cultured in M9 supplemented with 0.2% fructose. oligonucleotide primers, which anneals to the region 90 bp downstream with respect to the translation start site *fruR* (15 pmole each) was incubated with 1 unit of T4 polynucleotide kinase (NEB) in the presence of 30 μCi of [γ-^{32}P] ATP at 37˚C for 1h and purified with ProbeQuant™ (GE Healthcare). Primer anneals to the 25bp upstream of the

translation start site of *fruB* (50 pmole) were labelled with HEX. 150 μg of RNA samples were mixed with radioactive-isoptope-labelled primer and HEX-labelled primer in hybridization buffer (40 mM PIPES, pH 6.5, 400 mM NaCl and 1 mM EDTA), denatured at 95˚C for 3min and hyrbridized at 52˚C for 1hr. Reverse transcription was performed with RevertAid reverse transcriptase (Thermo Fisher Scientific) in the presence of RNaseOUT (Invitrogen). DNA and RNA were collected through phenol extraction and ethanol precipitation. To figure out the transcription start sites of *fruB* and *fruR*, a sequencing ladder was generated by using a Thermo Sequence Cycle Sequencing kit (USB) with the same primer used in annealing procedure.

10. Measurement of intracellular level of fructose metabolite

Quantification of metabolites using the Ion-pairing ultrahigh performance liquid chromatography (UPLC)-tandem mass spectrometry (MS/MS) was performed as previously described (Buescher *et al.*, 2010). The wild-type cells were grown at LB medium and washed with M9 medium in a same preparation manner as mentioned above. Each culture was divided into two identical samples, with one supplemented with 0.2% fructose and the other with 0.2% glucose. We adopted the fast centrifugation as a sampling method. 1 ml culture volume was centrifugated at 13,000 × g for 15 s. The cell pellet frozen at -80˚C until extraction. Samples extracted three times with 0.5 mL 60% (v/v) ethanol buffered with 10 mM ammonium acetate pH 7.2 at 78˚C for 1 min. After each extraction step, biomass was separated by centrifugation for 1 min at 13,000 × g. Seperation of hexose phosphates and mass spectrometric analysis of these compound was performed with LTQ Orbitrap Elite mass spectrometer (Thermo Scientific) equipped with a nano-electrospray source and a nanoAcquity UPLC system (Waters) in Korea Basic Science Institute (KBSI).

Table 2. Bacterial and plasmids used in this study.

Strains or plasmids	Genotypes and/or Descriptions	References or Source
Strains		
Vibrio cholerae		
O1 El Tor N16961		Lab stock
Δ*fruR*	N16961 Δ*fruR*	This study
Δ*fruB*	N16961 Δ*fruB*	This study
Δ*fruK*	N16961 Δ*fruK*	This study
Δ*fruA*	N16961 Δ*fruA*	This study
Δ*VC1821*	N16961 Δ*VC1821*	This study
Δ*VC1823*	N16961 Δ*VC1823*	This study
Δ*VC1825*	N16961 Δ*VC1825*	This study
Δ*VC1826*	N16961 Δ*VC1826*	Lab stock
Δ*lacZ*	N16961 Δ*lacZ*	Lab stock
Δ*fruR*Δ*lacZ*	N16961 Δ*fruR* Δ*lacZ*	This study
Escherichia coli		
ER2566	F^- λ^- *fhuA2* [*lon*] *ompT lacZ*::T7 gene 1 *gal sulA*11 Δ(*mcrC-mrr*)114::IS10 R(*mcr*-73::miniTn10-TetS)2 R(*zgb*-210::Tn10) (TetS) *endA1* [*dcm*]	New England Biolabs
BL21/pLysSRARE	F^- *ompT gal dcm lon hsdSB*(rB- mB-) λ (DE3) pLysSRARE(Cm^r)	Novagen
SM10/λpir	*thi thr leu tonA lacY supE recA*::RP4-2-Tc::Mu (λpir R6K) Km^r	(Miller & Mekalanos, 1988)
Plasmids		
pDM4	Suicide vector for homologous recombination into *V. cholerae* chromosome, OriR6K, Cm^r	(Milton *et al.*, 1996)
pET43.1a		Novagen
pET-VcFruR	pET43.1a-based expression vector for VcFruR, Amp^r	This study
pET-VcFruR(N73D)	pET43.1a-based expression vector for VcFruR(N73D), Amp^r	This study
pET-RpoD	pET43.1a-based expression vector for RpoD, Amp^r	Lab stock
pJK1113	pBAD24 with *oriT* of RP4 and *nptI*, P_{BAD}; Km^r, Amp^r	(Lim *et al.*, 2014)
pJK-Z	pJK1113-based expression vector containing promoter-less LacZ, Amp^r	Lab stock
pJK1113-BZ	pJK1113-based expression vector for LacZ under control of *fruB* promoter, Amp^r	This study
pJK1113-BZ-1C	pJK1113-BZ based expression vector containing mutated sequence at *fruB* O1, Amp^r	This study
pJK1113-BZ-2C	pJK1113-BZ based expression vector containing mutated sequence at *fruB* O2, Amp^r	This study
pJK1113-BZ-3C	pJK1113-BZ based expression vector containing mutated sequence at *fruB* O3, Amp^r	This study
pJK1113-BZ-1,2C	pJK1113-BZ based expression vector containing mutated sequence at *fruB* O1 and O2, Amp^r	This study
pJK1113-BZ-1,3C	pJK1113-BZ based expression vector containing mutated sequence at *fruB* O1 and O3, Amp^r	This study
pJK1113-BZ-2,3C	pJK1113-BZ based expression vector containing mutated sequence at *fruB* O2 and O3, Amp^r	This study
pJK1113-BZ-1,2,3C	pJK1113-BZ based expression vector containing mutated sequence at *fruB* O1, O2 and O3	This study
pDM4-BR	pDM4-based homologous recombination vector for duplicate the *fruR-fruBKA* intergenic region at *fruB*-side, Cm^r	This study
pDM4-BR-1C	pDM4-BR variants containing mutated sequence at *fruB* O1, Cm^r	This study
pDM4-BR-2C	pDM4-BR variants containing mutated sequence at *fruB* O2, Cm^r	This study

pDM4-BR-3C	pDM4-BR variants containing mutated sequence at *fruB* O3, Cm^r	This study
pDM4-BR-1,2C	pDM4-BR variants containing mutated sequence at *fruB* O1 and O2, Cm^r	This study
pDM4-BR-1,3C	pDM4-BR variants containing mutated sequence at *fruB* O1 and O3, Cm^r	This study
pDM4-BR-2,3C	pDM4-BR variants containing mutated sequence at *fruB* O2 and O3, Cm^r	This study
pDM4-BR-1,2,3C	pDM4-BR variants containing mutated sequence at *fruB* O1, O2 and O3, Cm^r	This study
pDM4-RB	pDM4-based homologous recombination vector for duplicate the *fruR-fruBKA* intergenic region at *fruR*-side, Cm^r	This study
pDM4-RB-1C	pDM4-RB variants containing mutated sequence at *fruB* O1, Cm^r	This study
pDM4-RB-2C	pDM4-RB variants containing mutated sequence at *fruB* O2, Cm^r	This study
pDM4-RB-3C	pDM4-RB variants containing mutated sequence at *fruB* O3, Cm^r	This study
pDM4-RB-1,2C	pDM4-RB variants containing mutated sequence at *fruB* O1 and O2, Cm^r	This study
pDM4-RB-1,3C	pDM4-RB variants containing mutated sequence at *fruB* O1 and O3, Cm^r	This study
pDM4-RB-2,3C	pDM4-RB variants containing mutated sequence at *fruB* O2 and O3, Cm^r	This study
pDM4-RB-1,2,3C	pDM4-RB variants containing mutated sequence at *fruB* O1, O2 and O3, Cm^r	This study
pJK1113(Chl.)	pBAD24 with *oriT* of RP4 and *nptI*, P_{BAD};Cm^r	(Lee *et al.*, 2018)
pJK1113-VcFruR	pJK1113(Chl.) based expression vector for *fruR*. Cm^r	This study
pACYC-184	A low copy number cloning vector; Cm^r Tet^r	(Chang & Cohen, 1978)
pACYC-VcFruR	pACYC based FruR expression vector under control of constitutive P_{cat} promoter	This study
pACYC-VcFruR(N73D)	pACYC based FruR(N73D) expression vector under control of constitutive P_{cat} promoter	This study
pACYC-VcFruR(R197E)	pACYC based FruR(R197E) expression vector under control of constitutive P_{cat} promoter	This study

Table 3. Oligonucleotides used in this study.

Name	Nucleotides sequence (5'-3')	Uses
fruR-d1F	AAAAAACTCGAGTTTGCCGTAGTGACGATCG (XhoI)	Construction of pDM4-based vector for in-frame deletion
fruR-d1R	CCTTTATTTTGTAAGGGGGTCTCGTTTTATG	
fruR-d2F	CGAGACCCCCTTACAAAATAAAGGTATG	
fruR-d2R	TTTTTTAGATCTGGATAAACCTGACGCAGC (BglII)	
fruB-d1F	AAAAAACTCGAGCGATGCGGCATGATCCGGCC (XhoI)	
fruB-d1R	TTTTTTCCATGGTCTTAACTCCTGTCTGCCTC (NcoI)	
fruB-d2F	AAAAAACCATGGGGGGCATCACATGACAAAAAAAG (NcoI)	
fruB-d2R	TTTTTTTCTAGACTTTTTTATTCATGCTGCGC (XbaI)	
fruK-d1F	AAAAAACTCGAGGTGTAATGACGTCCATCAGC (XhoI)	
fruK-d1R	TTTTTTGGATCCGTGATGCCCCTTAACCTTCG (BamHI)	
fruK-d2F	AAAAAAGGATCCGGACAGAAGGTCGTGAAGATG (BamHI)	
fruK-d2R	TTTTTTTCTAGACCACGCGTTTCAACTTTGATC (XbaI)	
fruA-d1F	AAAAAACTCGAGAACTGCGCAGCATGAATAAA (XhoI)	
fruA-d1R	TTTTTTCCATGGGACCTTCTGTCCTTAGGCAC (NcoI)	
fruA-d2F	AAAAAACCATGGTCTGAGTGCATGGTGAAAGG (NcoI)	
fruA-d2R	TTTTTTTCTAGAGACAACATTCGCAGTGAGGAG (XbaI)	
1821-d1F	AAAAAACTCGAGACATCCATTAATTTTAGCTC (XhoI)	
1821-d1R	TTTTTTCCATGGAATTTCACGCCTTATGATTG (NcoI)	
1821-d2F	AAAAAACCATGGACCTTAAGCTCCTCCCCCAG (NcoI)	
1821-d2R	TTTTTTTCTAGAATTCTTGGCACTATCGCCGG (XbaI)	
1823-d1F	AAAAAACTCGAGTGACCATCTTCTGCACCGTAATC (XhoI)	
1823-d1R	TTTTTTCCATGGGGAAATCCCTCATTGTTATTTTT (NcoI)	
1823-d2F	AAAAAACCATGGTCCTTGGCATGATGCATGAATTC (NcoI)	
1823-d2R	TTTTTTTCTAGATACGCAGGTGGAAGAGCGTTC (XbaI)	
1825-d1F	AAAAAATCTAGAGAATGCCGCTTTATCTGAAATTC (XbaI)	
1825-d1R	TGAAGCACGATAATCATGTAAACCCTCACTTCGTC	
1825-d2F	AGTGAGGGTTTACATGATTATCGTGCTTCAATTTA	
1825-d2R	TTTTTTCTCGAGATGAGTTCTCTAGCCTGCTCGCC (XhoI)	
BR-F	AGTGTCATCTCGAGAAGGGGGTCTCGTTTTATG (XhoI)	Construction of pDM4-BR or RB
BR-R	CACAATGGGGGCCCTTTGCCGTAGTGACGATCG (ApaI)	
RB-F	CACGGTTACTCGAGAAATGCTCACCATAACCTAG (XhoI)	
RB-R	AGTTCTAAGGGCCCCATTCTTAACTCCTGTCTGCC (ApaI)	
BZ-F	AAAAAAGTCGACAAGGGGGTCTCGTTTTATGTG(SalI)	Construction of pJK-BZ
BZ-R	TTTTTTGTCGACTCTTAACTCCTGTCTGCCTC(SalI)	
BR1C-F	TGAATTATACAGATCGTGAGTATTCGATTAAAGCTGAAAG GATTCAGCAAAAGTACCG	Introduction of mutated sequence into *fruR-fruBKA* intergenic region
BR 1C-R	CAGCTTTAATCGAATACTCACGATCTGTATAATTCAACACT AGGCTAGGATCAAAAATCG	
BR 2C-F	CAGTATTAAAAGATCGTGAGTATTCGAAAAGTACCGTTGA TTCACAATCTCGTC	
BR 2C-R	CGGTACTTTTCGAATACTCACGATCTTTTAATACTGAATCG ATTCAGCGTATAATTC	
BR 3C-F	TGCCCTTTGTAGATCGTGAGTATTCGTCAAAGGAAAACGA GACGGGATG	
BR 3C-R	TTTCCTTTGACGAATACTCACGATCTACAAAGGGCAAAAA AATTCAGC	
BR 1,2C-F	TGAATTATACAGATCGTGAGTATTCGATTAAAAGATCGTG AGTATTCGAAAAGTACCGTTGATTCACAATCTCGTC	
BR 1,2C-R	GATCCTAGCCTAGTGTTGAATTATACAGATCGTGAGTATTC GATTAAAAGATCGTGAGTATTCGAAAAGTACCG	
fruR-F	AAAAAACATATGACACTGG ATGAAATCGC (NdeI)	Construction of FruR expression plasmid
fruR-R	TTTTTTCTCGAGTTAAGTGCGCACCTTTAACTG (XhoI)	
fruR-F(pACYC)	AAAAAATCTAGAATGACACTGGATGAAATCGC (XbaI)	
fruR-R(pACYC)	TTTTTTCTGCAGTTAAGTGCGCACCTTTAACTG (PstI)	

N73D-F	TAATCATTCCGGATCTGGAAGACACCAGTT	
N73D-R	AAACGCGCATAACTGGTGTCTTCCAGATCC	
R197E-F	CAAACCCTTGTTCCTCTTCACGCGACACATTCA	EMSA
R197E-R	GTGTCGCGTGAAGAGGAACAAGGGTTTGCCAT	
BE-F	TTTTGATCCTAGCCTAGTGTTGAATTATAC	
BE-R	TTGTCATTCATCCCGTCTCGTTTTCCTTTG	
BE-F	6FAM-TTTTGATCCTAGCCTAGTGTTGAATTATAC	DNase1 footprinting
BE-F(L)	6FAM- TTGTCATTCATCCCGTCTCGTTTTCCTTTG	
rrsG-qRT-F	TTAGCCGGTGCTTCTTCTGT	qRT-PCR
rrsG-qRT-R	CAGCCACACTGGAACTGAGA	
fruR-qRT-F	AACTGAATGTGTCGCGTGAA	
fruR-qRT-R	CATCAATTCTGGCTGCTCAA	
fruB-qRT-F	GGGAACGATCACTGAGGAAA	
fruB-qRT-R	CATTGACGACTTGACCATCG	
fruK-qRT-F	GTGGCTTCACGAAAACCAAT	
fruK-qRT-R	TTACCGCAAGTGCAGACAAG	
fruA-qRT-F	GGAGCTCAGTAATGCCTTCG	
fruA-qRT-R	GAGAGCGCGATGATAAGACC	
1821-qRT-F	ACGTTCTGCTTCATGCTCCT	
1821-qRT-R	CTTCTGCGATTTCGTCTTCC	
1824-qRT-F	CACCAAATCTCTCGCGGTAT	
1824-qRT-R	GGCATAGTGCCATTTGACCT	
1825-qRT-F	TTGCGGGTGATTTTCATACA	
1825-qRT-R	CGGTATCCCAGTTCGGTTTA	
1826-qRT-F	GCTGAAGCACTGGAAAAAGG	
1826-qRT-R	GAATTGGCGCTTTCACATTT	
1332-qRT-F	CGCTGATGATCCCGATTACT	
1332-qRT-R	GCCAGTGAAGGAAGCGTAAG	
tss1-F	CTATTGCCTG CACGCAATGC	TSS mapping
tss1-R	GACACTGGATGAAATCGCGA	
tss2-F	TCGATTCAGTATTAAAGCTG	
tss2-R	GCTGAATCGGTTCAGCACAA	
tss3-F	AGGATTCAGCAAAAGTACCG	
tss3-R	ATACCTTGTCATTCATCCCG	
tss4-F	GTCAGATTGTGTCGAGTATC	
tss4-R	TGTCTGCCTCTATAGGCGAG	

* Engineered restriction sites were underlined with the corresponding restriction enzyme shown in parentheses.

Chapter III. Results

1. The VcFruR-mediated activation of the transcription of the *fruBKA* operon in the presence of fructose.

1.1 The fructose-mediated transcriptional regulation of PTS genes.

To figure out the fructose-mediated transcriptome changes, specifically to identify the global mRNA changes and to find the related transcription regulator, RNA sequencing was conducted with the RNAs extracted from *V. cholerae* cells cultured in minimal medium containing either 0.2% fructose or glucose and also from control cells grown without any carbon sources. To determine the regulons directly affected by the addition of fructose, any genes that are differentially expressed in glucose-grown cells compared to cells at no sugar medium were excluded from the fructose-regulated candidates. As a result, we found 12 genes that have dramatically increased (genes with an expression change >1.5, log2Fold) only in the fructose medium compared to no sugar medium and glucose supplemented medium. qRT-PCR experiment using gene specific primers was conducted to assess the validity of our results (Table 3).

1.2 Identification of the major transporter or metabolic enzyme for utilization of fructose

To identify the major transporter or metabolic enzyme for utilization of fructose among these putative fructose specific PTS genes (Figure 2), we generated each mutant strain that has in-frame deletion on the representative gene of the indicated PTS genes and grew these strains in the M9 medium supplemented with glucose or fructose. Among these mutants, the *fruB* and *fruA* mutant showed slight growth retardation compared to wild-type cells in the fructose medium. However, deletion mutants of *fruR* and *fruK* showed severe growth defect in fructose medium. The previous work demonstrated that deletion of *fruB* results in minor delay in growth in fructose medium but

Table 4. The list of genes differentially expressed when *V. cholerae* utilizes fructose as a sole carbon source.

gene	log2FoldChange (RNAseq)	log2FoldChange (qRT-PCR)	product
VC1332[a]	1.79	-2.22	hypothetical protein
VC1333[a]	1.7		hypothetical protein
VC1821	5.1	8.36	PTS system fructose-specific transporter subunit IIBC
VC1824	1.94	4.15	PTS system nitrogen regulatory subunit IIA
VC1825	3.3	7.71	transcriptional regulator
VC1826	6.56	10.43	PTS system fructose-specific transporter subunit IIABC
VCA0219	1.99	-1.39	hemolysin
VCA0516[a]	6.04	8.08	PTS system fructose-specific transporter subunit IIBC
VCA0517[a]	7.35		1-phosphofructokinase
VCA0518[a]	7.94		PTS system fructose-specific transporter subunit IIA/HPr protein
VCA0519	5.16	4.54	DNA-binding transcriptional regulator FruR
VCA0843	1.92	-0.77	glyceraldehyde-3-phosphate dehydrogenase

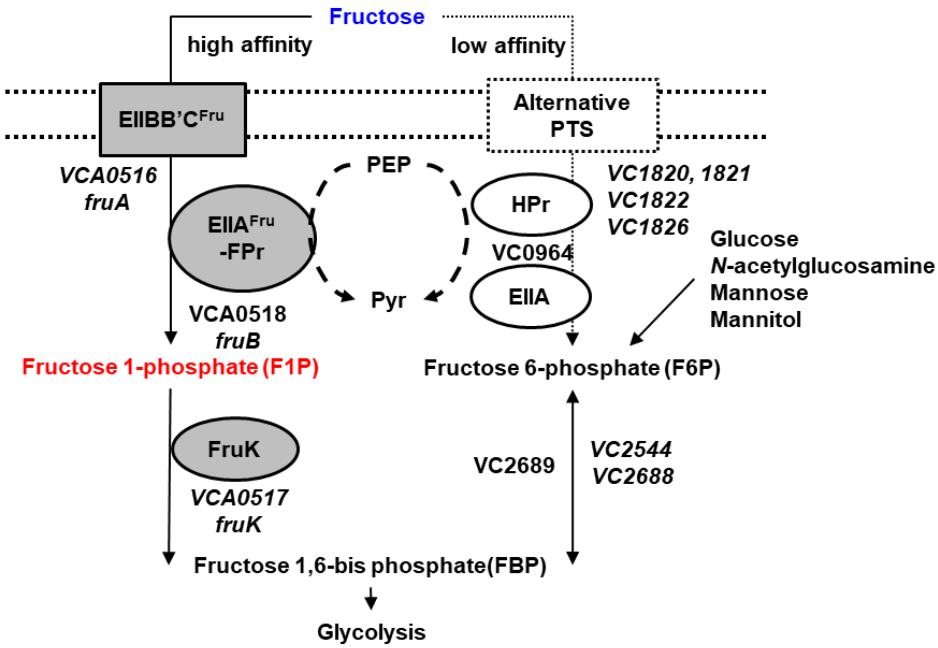

Figure 2. The schematics of fructose metabolism in *V. cholerae.*

Fructose is mainly transported through fructose-specific PTS (PTS^{Fru}) which consists of FruB ($FPr\text{-}IIA^{Fru}$) and FruA ($EIIBB'C^{Fru}$) components. Initial modified form of fructose is fructose 1-phosphate (F1P), which is then channeled towards glycolysis following the activity of 1-phosphofructokinase (FruK) to yield fructose 1,6-bisphosphate (FBP). PEP; Phosphoenolpyruvate, Pyr; Pyruvate, Fru; fructose, Glc; glucose.

the activity of HPr, which participates in the transport of most of PTS sugars restores the growth in fructose medium (Houot *et al.*, 2010a). The *fruA* mutant also displays marginal retardation of growth rate in fructose medium but the utilization of fructose was not affected (Hayes *et al.*, 2017). As expected, deletion of the alternative PTS (VC1821, 1823, 1826) and transcription factor, VC1825 had no effect on their growth in fructose medium. All mutant strains grew similar to the wild type in glucose-supplemented medium (Figure 3).

1.3 VcFruR-dependent activation of the transcription of the *fruBKA* operon

Since the genomic distribution of transcription regulator near the target metabolic genes is quite common in diverse bacterial species (Kornberg, 2001), we speculated that the deletion of VcFruR which is encoded in VCA0519 (*fruR*) might be linked to the deactivation of transcription of the *fruBKA* operon. A qRT-PCR experiment using primers covering each target genes represents that expression of *fruR* is essential for the expression of the *fruBKA* operon in the presence of fructose (Figure 4).

1.4 Intracellular F1P only exists when cell utilizes fructose.

FBP is generated when the cell utilizes the variety of PTS sugars. It is reported that intracellular level of FBP changes ranging from 5 mM to 15 mM responding to metabolic flux (Bennett *et al.*, 2009). However, intracellular F1P only exists when the fructose translocates through PTS^{Fru}, and the intracellular concentration reaches almost 0.2 mM in the fructose grown cultured medium (Chavarria *et al.*, 2013). To unravel the correlation between intracellular level of fructose derivatives and the expression of PTS^{Fru}, we measured the intracellular level of fructose derivatives from the cells grown

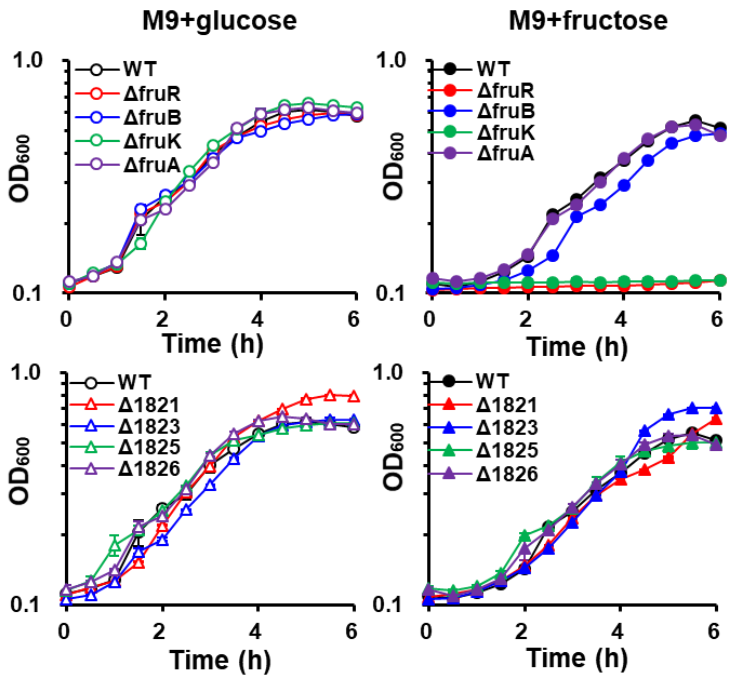

Figure 3. Growth defect of the *fruR* and *fruK* mutants on fructose

Growth curves of *fruB*, *fruK* and *fruA* mutants (upper panels) and mutants of alternative PTS components (lower panels) in M9 medium supplemented with 0.2% glucose (left panels) or fructose (right panels). Optical density of cultures was measured at 600nm using a multimode microplate reader (TECAN). The mean and standard deviation value of three independent measurements are shown for each experiment.

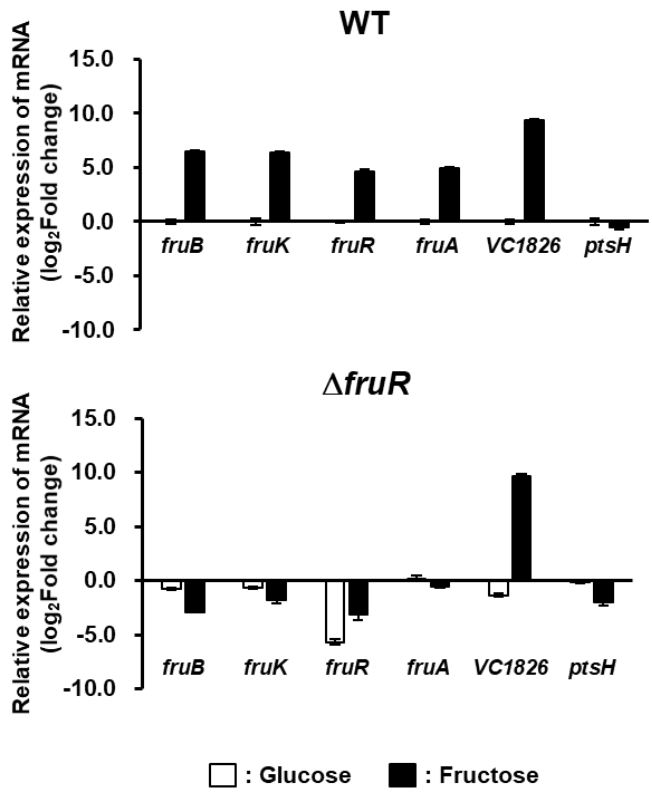

Figure 4. The relative mRNA expression of the *fruBKA* operon in a Δ*fruR*

The relative mRNA expression of the indicated genes in the wild type and a *fruR* mutant cultured in M9 medium supplemented with 0.2% of glucose or fructose. Each mRNA expression level of genes is shown relative to the corresponding value of the wild type cultured on glucose. The mean and standard deviation of three independent measurements are shown.

in the absence (supplemented with glucose as a carbon source) or presence of fructose-supplemented minimal medium (Figure 5). We found that F1P concentration was high in the wild-type cells cultured in fructose medium in contrast to those detected in *V. cholerae* cells cultured in glucose medium. The concentrations of other fructose derivatives, F6P and FBP, did not show significant difference.

2. VcFruR forms homo-dimer

2.1 Aminoacid sequence alignment of FruR in diverse baceteria

VcFruR has 47% amino acid sequence identity with EcFruR which has a conserved DNA binding domain and an effector binding domain. However, the leucine-mini-zipper domain that structurally determines the tetrameric state of the protein is absent in VcFruR (Weickert & Adhya, 1992) (Figure 6).

2.2 Determination of oligomeric state of VcFruR

Gel filtration experiment was performed to determine the oligomeric state of VcFruR. The elution volume of VcFruR corresponded to a molecular mass about 71.82 kDa, as estimated from the calibration curve obtained with molecular protein standard marker. This means that while EcFruR forms a tetramer (Cortay *et al.*, 1994), the native VcFruR exists as dimer in the solution (Figure 7), implying that the regulatory mechanism of VcFruR might be different from that of EcFruR.

3. The direct binding of VcFruR to three operators in *fruR-fruBKA* intergenic regions inducing DNA bending

3.1 Searching for the VcFruR binding sites in *V. cholerae* chromosomes

EcFruR directly binds to the 14-bp-long FruR box with

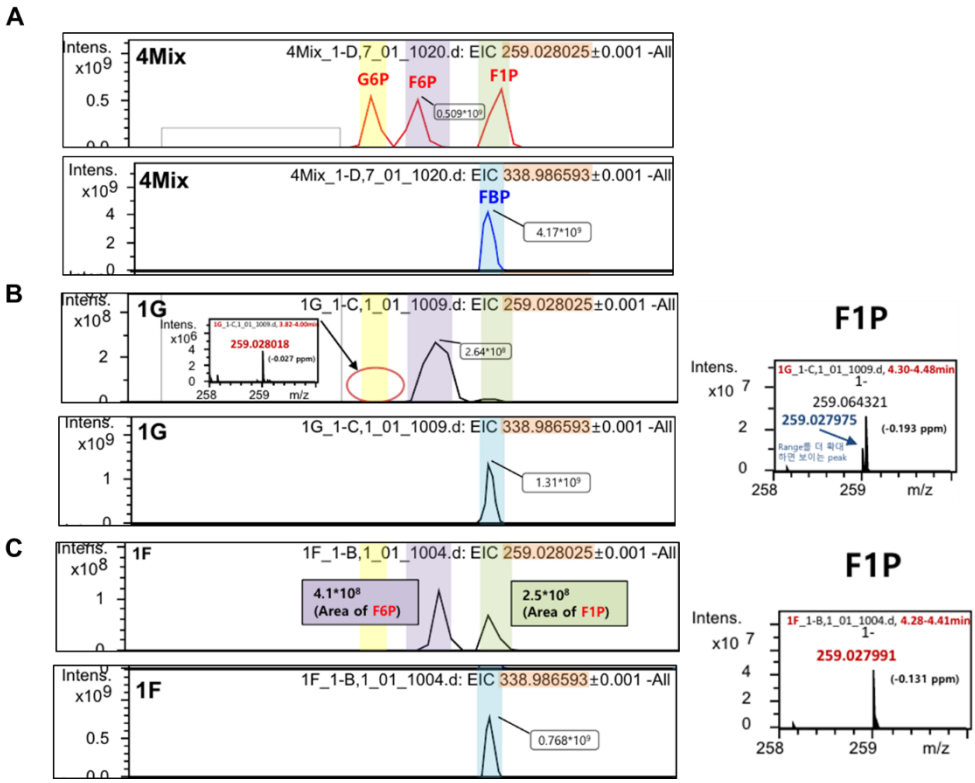

Figure 5. Measurement of intracellular level of fructose metabolites

Ion-pairing ultrahigh performance liquid chromatography (UPLC)-tandem mass spectrometry (MS/MS) was perform with the cell extract from the cell cultured in minimal medium supplemented with glucose or fructose.

(A) Standard solution containing each 10 μM of G6P, F6P, F1P and FBP was separated by the combination of LC and MS/MS. Each compounds are basedline separated by UPLC. Thre retention times of each compound are 3.9 min (G6P), 4.1 min (F6P), 4.3 min (F1P) and 6.9 min (FBP). **(B)** Extracted ion chromatogram (EIC) of glucose-grown cell and **(C)** of fructose-grown cell are shown. Samples were prepared by fast centrifugation method (Buescher *et al.*, 2010) and extracted three times with 0.5 mL of 60% (v/v) ethanol buffered with 10 mM ammonium acetate pH 7.2 at 78˚C for 1 min.

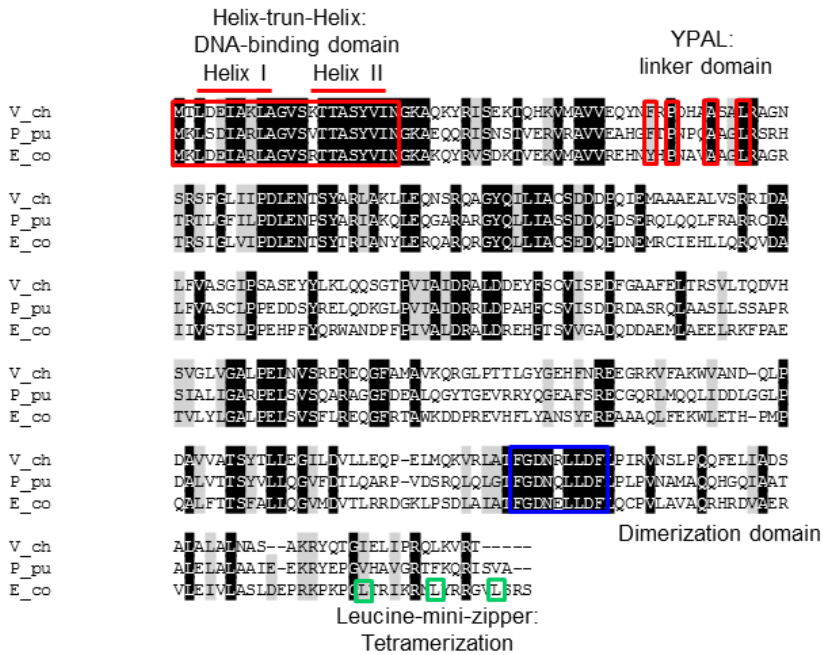

Figure 6. Multiple amino acid sequence alignment of FruR orthlogs in three species in *Gammaproteobacteria*.

The amino acid sequences conserved in FruR orthologs in three different species (*E. coli*, *P. putida* and *V. cholerae*) are highlighted with black. Conserved amino acids sequences of helix-turn-helix motif, dimerization domain and leucine-zipper domain are marked with red, blue and green boxes, respectively. V_ch; *V. choleare* El Tor N16961, P_pu; *P. putida* KT2440, E_co; *E. coli* K-12 MG1655.

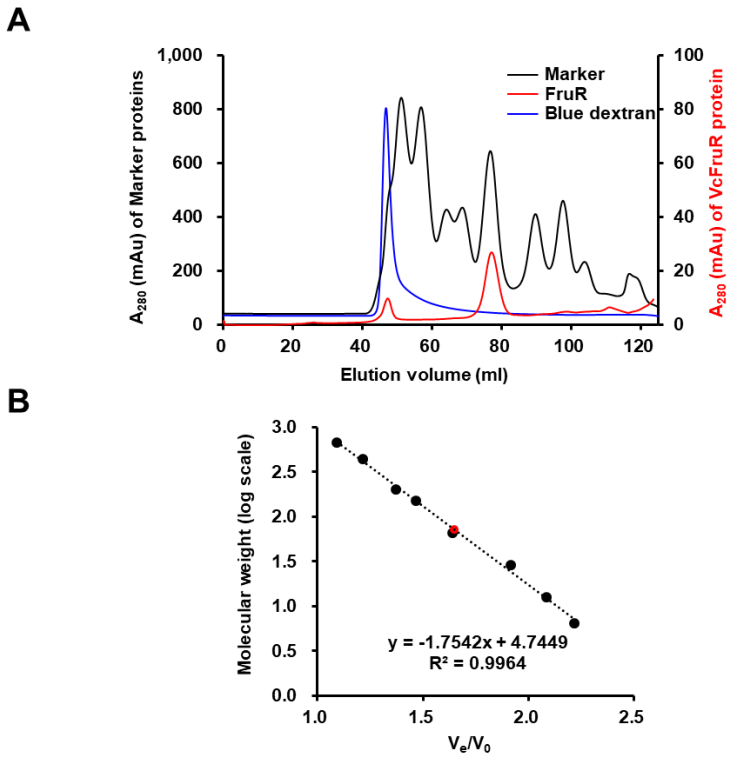

Figure 7. Determination of the oligomeric state of VcFruR

(A) Gel filtration chromatography of VcFruR, the red line indicates chromatogram of the VcFruR. Nine molecular weight markers (Black line) and Blue dextran (Blue line) were used to calibrate the Superdex 200 pg column (GE Healthcare Life Sciences). **(B)** The molecular mass was plotted versus the V_e/V_0 value, where V_e, is the elution volume and V_0, is the void volume, as determined from the elution of blue dextran. Red dot indicates the estimated molecular weight of the dimeric state of VcFruR.

imperfect palindromic sequence (5'-GCTGAAnC/GnTTCA-3') (Shimada *et al.*, 2011). Based on the EcFruR binding sites, we searched for the putative VcFruR binding sites on the two *V. cholerae* chromosomes using the PRODORICS software (Table 4.)(Munch *et al.*, 2005). Fourty sites were detected in the intergenic or untranslated regions (UTRs). Then, the putative VcFruR regulon was compared with aforementioned RNAseq data (Table 3). As a result, we identified only three binding sites in whole genome and only four target genes were predicted as a VcFruR regulon.

3.2 Direct binding of VcFruR to only three operators located in *fruR-fruBKA* intergenic region.

Three binding sites are located in the 338-bp-long intergenic region of *fruR*(449421)-*fruB*(449082), herein each binding sites are named with *fruB* O1, O2 and O3, centered at 258.5 bp, 236.5 bp and 109.5 bp from the start codon of *fruB*, respectively (Figure 8). Each operator has 16-bp sequences similar to the known EcFruR consensus sequences (Figure 8, lower panel)(Shimada *et al.*, 2011). To confirm whether VcFruR can bind to each cognate operators, EMSA was performed. EMSA using the DNA fragment covering entire *fruR-fruBKA* intergenic region as a probe demonstrated that three DNA-VcFruR complexes were detected as DNA-bound VcFruR increases (Figure 9)

3.3 Sequenctial binding of VcFruR to three operators.

To figure out which operator(s) is/are occupied with VcFruR in each of the three DNA-VcFruR complexes, DNA fragment containing different combination of mutation on the operator sequences that VcFruR cannot bind

Table 5. The list of putative VcFruR binding sites on two chromosomes of *V. cholerae*

	Start	End	Strand	Sequence	Gene Name	ATG-Distance	Location
	1212283	1212294	-	TGAATCGCTATT	VC1142	77	intergenic
	1212283	1212294	-	TGAATCGCTATT	VC1143	376	intergenic
	1736343	1736354	+	TGAATCGTTATC	-	-	non-coding region between gene VC1619 and VC1621
	1712537	1712548	+	TGAATCGTTTGG	VC1599	193	intergenic
	1712537	1712548	+	TGAATCGTTTGG	tRNA-Val-2	68	intergenic
	463182	463193	-	TGAATCGATTGT	-	-	non-coding region between gene VC0432 and VC0433
	1387272	1387283	+	TGAATGGCTTAT	VC1306	190	intergenic
	1776647	1776658	-	TGAATGGTTTAG	VC1649	157	intergenic
	1776647	1776658	-	TGAATGGTTTAG	VC1650	160	intergenic
	543115	543126	+	TGAAACGCTTTC	-	-	non-coding region between gene VC0512 and VC0513
	2328822	2328833	-	TGAAACGCTTTC	VC2184	103	intergenic
	226205	226216	+	TGAAACGATTTG	VC0218	13	intergenic
	2328841	2328852	+	TGAAGCGCTTTT	VC2184	84	intergenic
	2493425	2493436	+	TGAACCGCTTAG	VC2341	155	intergenic
	612634	612645	-	TGAACCGTTTAG	-	-	non-coding region between gene VC0582 and VC0584
chromosome I	2906672	2906683	-	TGAACCGTTTAG	-	-	non-coding region between gene VC2732 and VC2734
	1859385	1859396	+	TGAAGCGCTTTA	VC1721	125	intergenic
	2749661	2749672	-	TGAAACGTTTAG	VC2567	151	intergenic
	2749661	2749672	-	TGAAACGTTTAG	VC2568	49	intergenic
	2005062	2005073	-	TGAAGCGTTTCT	VC1865	62	intergenic
	1625408	1625419	+	TGAATCGATTTG	-	-	non-coding region between gene VC1512 and VC1514
	845213	845224	-	TGAAGCGATTCA	VC0789	61	intergenic
	533476	533487	+	TGAATCGTTTTG	-	-	non-coding region between gene VC0498 and VC0502
	2845184	2845195	-	TGAATCGTTTTC	VC2677	139	intergenic
	1877843	1877854	+	TGAATCGGTTAG	VC1740	44	intergenic
	1951367	1951378	-	TGAAACGTTTAA	VC1808	293	intergenic
	136930	136941	-	TGAATCGCTTTA	VC0146	180	intergenic
	136930	136941	-	TGAATCGCTTTA	VC0147	13	intergenic
	845213	845224	+	TGAATCGCTTCA	VC0789	61	intergenic
	2490823	2490834	+	TGAATCGATTCA	VC2339	125	intergenic
	2490823	2490834	-	TGAATCGATTCA	VC2339	125	intergenic
	546303	546314	+	TGAAGCGATACA	VCA0608	167	intergenic
	546303	546314	+	TGAAGCGATACA	VCA0609	17	intergenic
	840790	840801	+	TGAATGGGTTAT	-	-	non-coding region between gene VCA0886 and VCA0888
	485516	485527	-	TGAATCGGTAAC	VCA0547	13	intergenic
	926	937	+	TGAATGGCTTAA	VCA0002	197	intergenic
	297942	297953	-	TGAAGCGATTTG	VCA0278	329	intergenic
	297942	297953	-	TGAAGCGATTTG	VCA0279	48	intergenic
	840671	840682	+	TGAAACGCTTTT	-	-	non-coding region between gene VCA0886 and VCA0888
	899077	899088	-	TGAACCGATTCG	VCA0947	118	intergenic
	97528	97539	+	TGAACCGTTTCT	-	-	non-coding region between gene VCA0087 and VCA0088
	1060997	1061008	-	TGAAGCGATTAA	-	-	non-coding region between gene VCA1103 and VCA1105
chromosome II	449186	449197	-	TGAACCGATTCA	**VCA0518**	104	intergenic
	449186	449197	-	TGAACCGATTCA	**VCA0519**	224	intergenic
	616183	616194	+	TGAATCGATTTT	-	-	non-coding region between gene VCA0680 and VCA0681
	1026193	1026204	-	TGAATCGCTTAG	-	-	non-coding region between gene VCA1072 and VCA1074
	987454	987465	+	TGAATCGCTTCG	-	-	non-coding region between gene VCA1035 and VCA1037
	449186	449197	+	TGAATCGGTTCA	**VCA0518**	104	intergenic
	449186	449197	+	TGAATCGGTTCA	**VCA0519**	224	intergenic
	449335	449346	+	TGAATCGATTCA	**VCA0518**	253	intergenic
	449335	449346	+	TGAATCGATTCA	**VCA0519**	75	intergenic
	449335	449346	-	TGAATCGATTCA	**VCA0518**	253	intergenic
	449335	449346	-	TGAATCGATTCA	**VCA0519**	75	intergenic

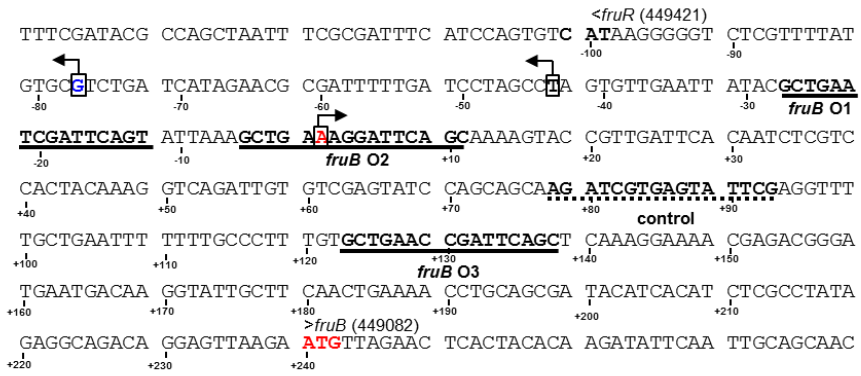

Consensus: $g_1c_2\mathbf{T_3G_4A_5A_6}t_7\mathbf{C_8}\text{-}\mathbf{G_8},a_7,\mathbf{T_6},\mathbf{T_5},\mathbf{C_4},\mathbf{A_3},g_2,c_1,$

Ec*fruB* O1:	CT**TGAA**AC-G**TTTCA**GC
Ec*fruB* O2:	GC**TGAA**TC-G**TTTCA**AT
Vc*fruB* O1:	GC**TGAA**TC-G**ATTCA**GT
Vc*fruB* O2:	GC**G**GAA**A**G-G**ATTCA**GC
Vc*fruB* O3:	GC**TGAA**CC-G**ATTCA**GC

Figure 8. Three VcFruR binding sites are located in *fruR-fruBKA* intergenic region

Three operators recognized by VcFruR are underlined with solid lines. The control sequences introduced to mutate each operator are underlined with dotted lines. The transcription start site (TSS) of *fruB* is marked with red letter in square box and a curved arrow. The TSSs of *fruR* are marked with blue letters in square boxes and curved arrows. The sequences of *fruB* operators (Vc*fruB* O1, O2 and O3) are aligned with EcFruR consensus sequence with numberings as previously described (Negre *et al.*, 1996), and with the nucleotide sequences of two *fruB* operators in *E. coli* (Ec*fruB* O1, O2) (lower panel). Black bold letters indicate the nucleotide sequences essential for the FruR binding to DNA. Blue and red bold letters indicate the difference in nucleotides between two or three Vc*fruB* operators.

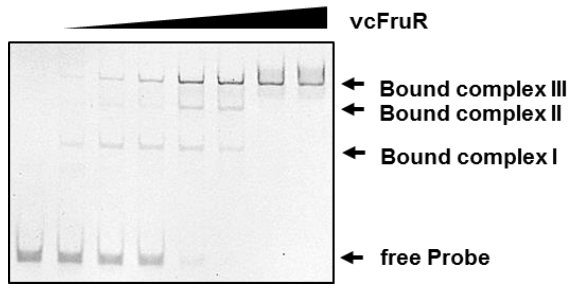

Figure 9. Direct binding of VcFruR to three operators in *fruR-fruBKA* intergenic region

EMSA using 338-bp DNA fragment covering the entire *fruR-fruBKA* intergenic sequence as a probe is shown. 60 ng of probes were incubated with increasing amount of VcFruR (0-180 ng) in buffer containing 10 mM Tris-HCl (pH 8.0), 5 % v/v Glycerol, 0.1 mM EDTA, and 1 mM DTT (TGED buffer). Each sample was incubated at 37˚C for 10 min and then analysed by a 6% Native PAGE in TBE gel followed by staining with EtBr. The arrows indicate the bands for the DNA-VcFruR complexes (Complex I, II and III) with different mobilities relative to that of the free probe.

bound to *fruB* O1 and O3, and complex III is the form of VcFruR bound to all three operators (Figure 10, lower figure). DNase1 footprinting with the DNA fragment covering entire *fruR-fruBKA* intergenic region mapped the VcFruR binding sites and indicated that VcFruR has high affinity to *fruB* O3 than other two operators (Figure 11). Relatively lower affinity of VcFruR to *fruB* O2 than other operators was quite reasonable because the sequence of O2 do not have the conserved sequence 5'-AAnC-3' at position at 5 to 8 (5'-AAAG-3'), which determines the binding specificity of FruR to the DNA (Negre *et al.*, 1996).

3.4 DNA bending induced by VcFruR binding to operators.

DNA morphological changes are accompanied by the direct transcription factor binding to a target DNA. To test whether the VcFruR binding to operators induces morphological changes of DNA, gel permutation assay was conducted. After EMSAs using 215-bp probes, which harbor only one each operator at different location (Figure 12), the respective mobilities of VcFruR bound DNA was plotted versus the relative distance between the 5' end of the fragment and the center of the binding site (Figure 12, lower panel). The bending angles in the each VcFruR bound operator are about 90˚.

4. Identification of transcription start sites (TSS) of the *fruB* and *fruR*

The previous work performed TSS-seq with *V. cholerae* cultured at LB medium and the TSS of the *fruBKA* operon were identified (Papenfort *et al.*, 2015). The TSS is located 241-bp upstream of the start codon of

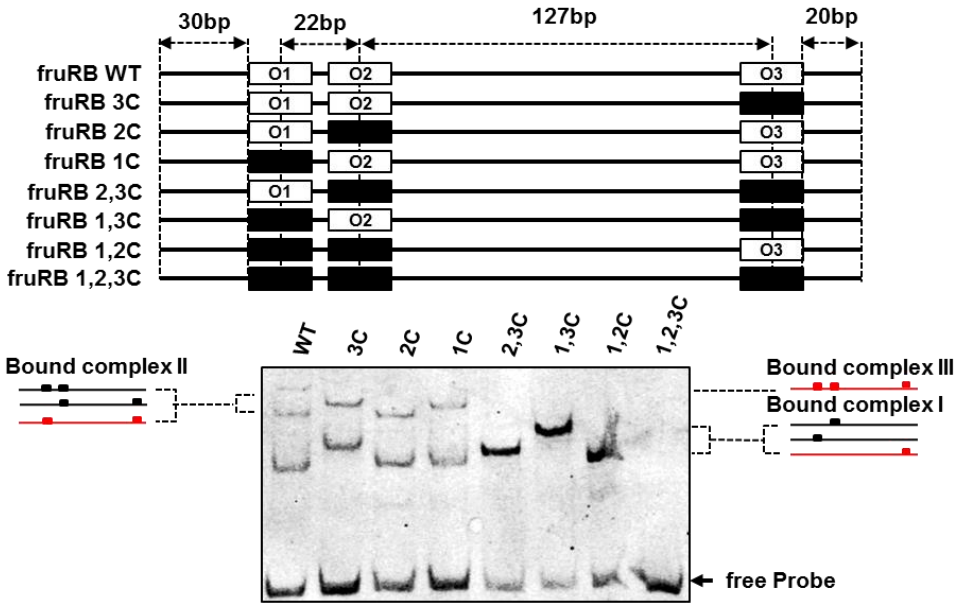

Figure 10. VcFruR sequentially binds to three operators

A line diagram of the *fruR-fruBKA* construct containing different combinations of mutated and wild-type sequences are shown (upper panel). Mutated sequences are indicated with filled black boxes. EMSA using these set of probes are shown (lower panel). Each probe (60 ng) was incubated with 60 ng of VcFruR in TGED buffer. The proposed mode of VcFruR binding to operators are indicated with red symbols. Filled square indicates the operator bound VcFruR.

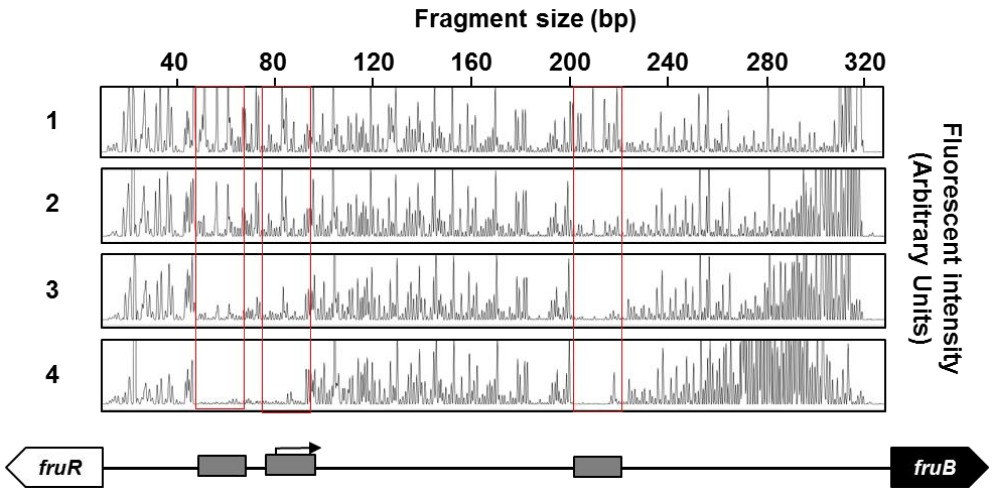

Figure 11. Mapping of the VcFruR-bidning sites in the *fruR-fruBKA* intergenic region.

DNase1 footprinting of VcFruR binding sites at the *fruR-fruBKA* intergenic region. A 200 ng of 338-bp DNA fragment covering the entire *fruR-fruBKA* intergenic region was fluorescently labeled with 6-Carboxyfluorescein (6-FAM) and incubated with increasing amount of purified VcFruR prior to digestion with DNase I. Lane 1-4 contain increasing amount of VcFruR (0, 100, 200 and 400 ng, respectively). The DNA regions corresponding to *fruB* O1, O2 and O3 are marked with red lines. The electropherograms of fluorescent peaks were aligned with manually generated sequence using GeneMapper software (Applied Biosystem). Curved arrow indicates the TSS of the *fruBKA* operon.

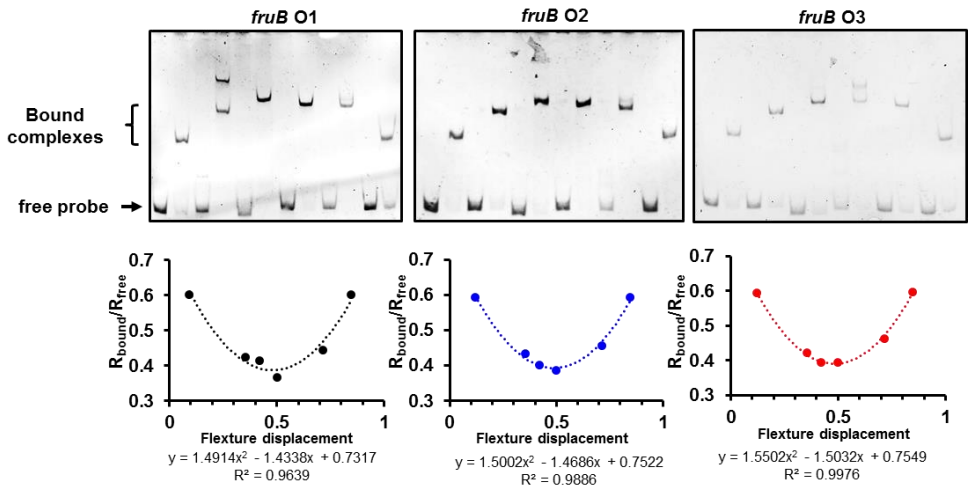

Figure 12. DNA bending induced by VcFruR binding to each operator

Gel permutation assay was conducted to investigate whether the binding of the VcFruR induces DNA bending at each *fruB* operator. After EMSA using 150-bp probes which harbor one of the three operators, which are located in different position at the DNA fragment, the distances between 5' end of the fragment and the center of the binding site (14, 53, 64, 75, 107 and 127 bp, respectively) were normalized to the full length of the probe DNA, called a flexure displacement. The band mobilities of VcFruR-DNA complexes on the gel (R_{bound}) relative to that of free probe (R_{free}), R_{bound}/R_{free}, which is denoted as "y" was plotted against the flexure displacement, which is denoted as "x". The resulting plot was fitted to a quadratic equation: $y = ax^2 - bx + c$. Bending angle α is given by the equation, $a = -b = 2c(1-\cos\alpha)$.

the *fruB*, which corresponded to the sixth nucleotide of the *fruB* O2 (Figure 8). To confirm the genuine TSS(s) of the *fruBKA* operon, RNAs from wild-type cells cultured on fructose and glucose were subjected to qRT-PCR analysis using the specific internal primers within the *fruR-fruBKA* intergenic region and the open reading frame (ORF) region of the *fruB* (Figure 13). We found that in the presence of fructose, 5' end of the *fruBKA* transcript is the previously reported TSS. We also performed the primer extension assay to map out the TSS(s) of *fruR*. As a result, we found that TSSs of *fruR* is located at 23-bp and 56-bp upstream of the start codon of *fruR* (Figure 14). The -10 and -35 regions of the promoter of the *fruB* and *fruR* were in good agreement with the sequence motif associated with σ70 binding (-35 motif: TTGnnn, -10 motif: TAnAAT), as previously described in *V. cholerae* (Manneh-Roussel *et al.*, 2018)

5. The effect of VcFruR binding to each *fruB* operators on the expression of the *fruBKA* operon

5.1. VcFruR bound on *fruB* O1 is essential for the activation of the *fruB* promoter.

Since VcFruR binds to the *fruB* O3 located 129.5-bp downstream of TSS with higher affinity than those of other operators, VcFruR was seen to act as a canonical transcriptional repressor. By contrast, since the deletion of *fruR* results in the growth defect on fructose and poor expression of the *fruBKA* operon, phenotypic evidences demonstrate that the role of VcFruR is close to an activator, not a repressor. To clarify the regulatory role of VcFruR on the expression of the *fruBKA* operon, we measured the *in vivo* promoter activity of *fruBKA* in the presence or absence of VcFruR. *V. cholerae* Δ*lacZ* strain were transformed with the pBAD based multi-copy plasmid containing *lacZ* transcriptional fusion with 338-bp of *fruB* promoter. The β-galactosidase

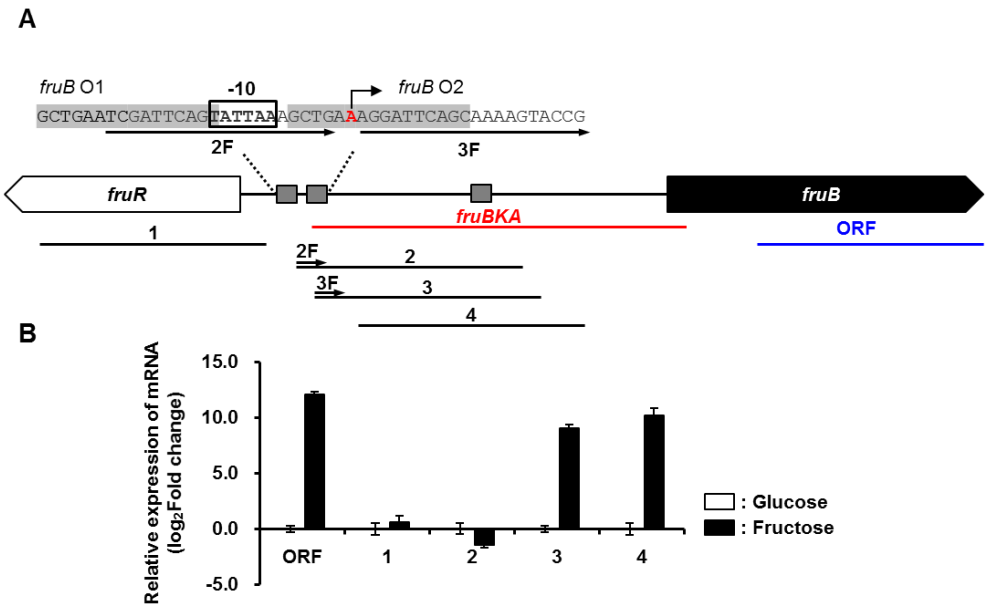

Figure 13. Mapping of TSS of the *fruBKA* operon by qRT-PCR

(A) Schematic representation of the *fruR-fruBKA* intergenic region. The ORFs of *fruR* and *fruB* are indicated with white box and black box, respectively, and the *fruB* O1, O2 and O3 are indicated with gray boxes. The characters shaded in gray are the sequences corresponding to *fruB* O1 and O2, and the TSS is colored in red. The black lines with numbers are RT-PCR product analyzed in (B). Blue line indicates the RT-PCR product in the ORF region. Red line indicates the *fruBKA* mRNA transcribed from the TSS. The primers used for the amplification of the "2" and "3" product (2F and 3F, respectively) are indicated with arrows.

(B) The relative amounts of RT-PCR products indicated in (A) in fructose-grown cells are shown. The data are shown relative to the corresponding values of cell cultured on glucose.

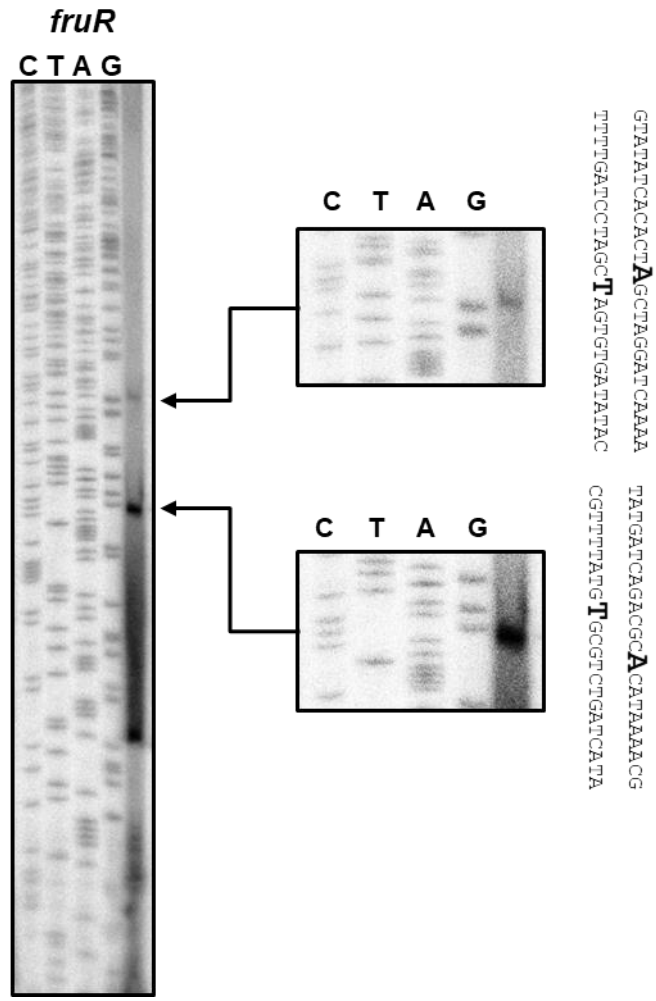

Figure 14. Mapping of TSSs of a *fruR* by primer extension

One hundred micrograms of RNA extracted from the *V. cholerae* cell cultured on fructose was mixed with radioactive-isoptope-labelled primers ([γ-^{32}P] ATP) which anneals to the region from 90-bp down stream from the translation start site of *fruR*. Lanes C, T, A and G represent the nucleotide sequencing ladders generated with the same primer. The arrow indicate the transcription start sites of the *fruR*.

activities were measured with the cell cultured in minimal medium containing glucose or fructose as a sole carbon source. As a result, fructose-grown cell exhibits 4-fold increase in β- galactosidase activity than the glucose-grown cell. However, isogenic mutant containing the plasmid carrying promoter-less *lacZ* and Δ*fruR*Δ*lacZ* mutant containing the wild-type *fruB* promoter fused with *lacZ* have no induction effect in the same condition (Figure 15). To identify which operator(s) is/are occupied by VcFruR when the transcription of the *fruBKA* operon is activated, we performed the β-galactosidase assay with the construct carrying the *fruB*-promoter containing different combination of mutated sequences (Figure 15). As a result, the strain with promoter containing the mutated sequence at the *fruB* O1 site (1C, 1,2C, 1,3C and 1,2,3C) exhibited no β-galactosidase activity. Strain harboring *lacZ* fused with wild-type *fruB* promoter has about 500 miller units of β-galactosidase activity at glucose medium but strains harboring *lacZ* fused with promoter mutation on the *fruB* O1 showed little activity (<100 miller units) in both glucose and fructose medium. A 2,3C mutant showed a little but significant increase in β-galactosidase activities in glucose medium than that of strain harbouring the lacZ fused with wild-type *fruB* promoter. As a result, we concluded that VcFruR binding to *fruB* O1 is essential for the activation of transcription of the *fruBKA* operon in the presence of fructose and *fruB* O2 and O3 are involved in transcriptional repression of the *fruBKA* in the presence of the glucose.

5.2 The regulatory effect of VcFruR bound on operator(s) on the expression of the *fruBKA* operon and *fruR*.

5.2.1 Construction of strains that have chromosomal duplication of *fruR*-*fruBKA* intergenic sequences.

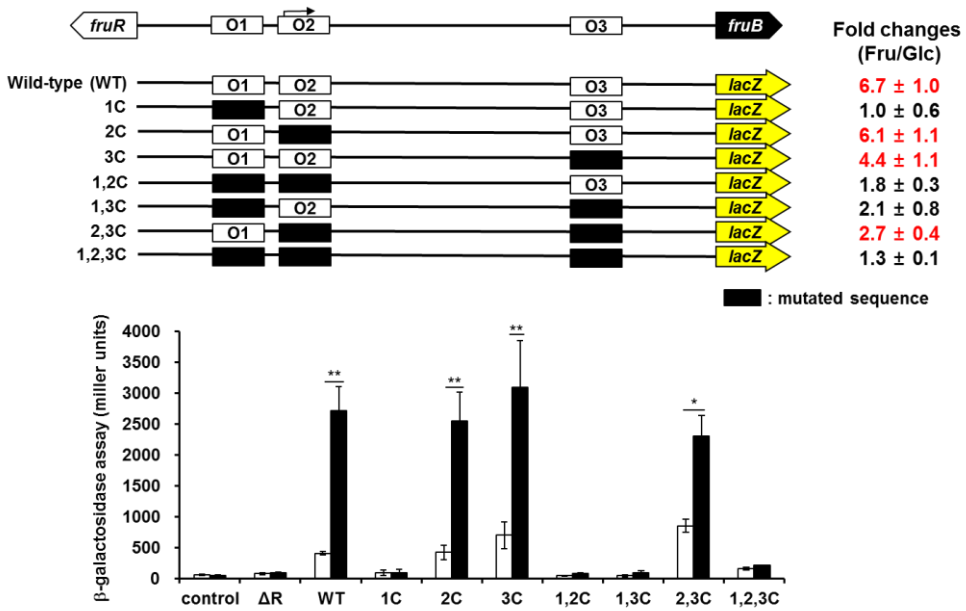

Figure 15. VcFruR binding to *fruB* O1 is indispensable for the activation of the transcription of the *fruB* promoter.

A line diagram of the promoter containing the wild-type or a mutated sequence used for the transcriptional fusion to *lacZ* is presented in the upper panel. The *V. cholerae* Δ*lacZ* strain was transformed with the plasmid carrying the *E. coli lacZ* gene transcriptionally fused with the wild-type *fruB* (WT) or a mutated promoter. An isogenic strain carrying the plasmid containing promoter-less *lacZ* was served as a negative control (control). The Δ*fruR*Δ*lacZ* strain transformed with BZ was indicated as ΔR. Indicated strains were treated with 0.2% glucose or fructose and then lysed to measure the β-galactosidase activity. The mean and standard deviation of three independent measurements are shown. Statistical significance was determined using Student's t test (*: *p*-value <0.05 and **: *p*-value<0.01).

Since *fruB* O1 positioned at the proximal to *fruR* ORF (23.5 and 57.5-bp upstream of each TSS), we wondered if the VcFruR bound at *fruB* O1 has regulatory effect on the mRNA expression of *fruR* itself. To distinguish the VcFruR bound *fruB* O1 effect on the expression of *fruBKA* operon from the effect on the expression of *fruR*, we generate the strains that duplicated the *fruR-fruBKA* intergenic sequences at the cognate *fruR* or *fruB*-side region of chromosome (Figure 16).

5.2.2 VcFruR binding to *fruB* O1 at the *fruB*-side is indispensable for the activation of the *fruBKA* operon.

We found that mutation on the operators in the *fruR*-side has no effect on the activation of transcription of *fruR* itself and the *fruBKA* operon (Figure 17). There is also little correlation between the extent of increased level of *fruR* expression and the increased level of *fruB* (Figure 17). However, mutation on the *fruB* O1 at the *fruB*-side promoter induces the growth retardation at the minimal medium containing fructose as a sole carbon source and at the same time leads to poor induction of *fruBKA* operon compared to the cell grown at the minimal media containing glucose (Figure 18). Strains with mutated sequences at the *fruB* O2 and/or O3 at the *fruB* side exhibited no defects in growth on fructose medium and induction of *fruB* (Figure 18).

6. The weakened binding ability of VcFruR to *fruB* O1 induced by F1P binding.

6.1 Identification of the genuine metabolite effector of VcFruR

To assess which metabolite acts as an effector of VcFruR, we supplemented 2 mM of diverse glycolytic metabolites including FBP and F1P with the DNA- FruR mixture and performed EMSA (Figure 19).

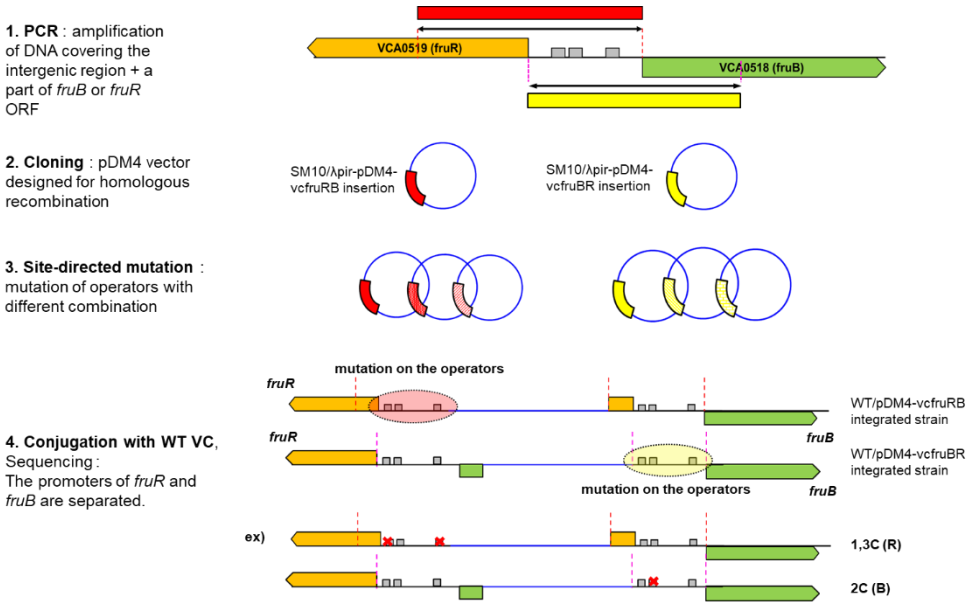

Figure 16. Schematics of the construction of strains with chromosomal duplication of *fruR-fruBKA* intergenic sequences.

A wild-type or mutated form of the *fruR-fruBKA* intergenic region including a part of the *fruR* ORF (red bar) or the *fruB* ORF (yellow bar) was chromosomally integrated by recombination using pDM4-based cloning to generate a strain in which the intergenic sequence was duplicated on the *fruR* or *fruB* side, respectively.'1,3C (B)' indicates the strain in which the operators O1 and O3 in the *fruB* side were mutated to the control sequence.

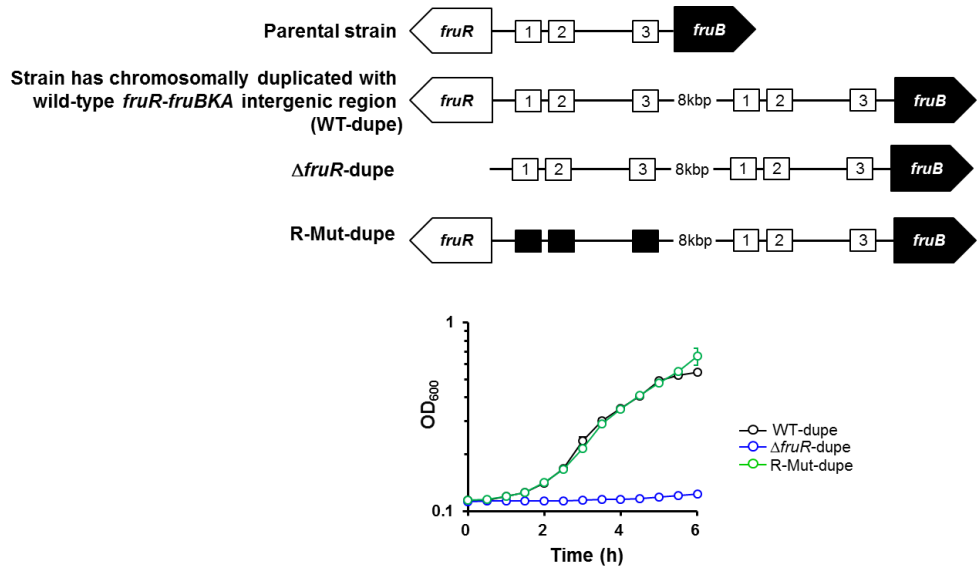

strain	The relative mRNA expression of *fruB*	The relative mRNA expression of *fruR*
WT	6.34 ± 0.28	5.85 ± 0.28
R-mut-dupe	7.98 ± 0.17	4.08 ± 0.16
Δ*fruR*-dupe	0.53 ± 0.13	-

Figure 17. FruR does not directly regulate the transcription of *fruR*

Wild-type *V. choleare* with chromosomal duplication of the wild-type *fruR-fruBKA* intergenic region (WT-dupe) and duplication of the mutated *fruR-fruBKA* intergenic region at *fruR*-side (R-Mut dupe) were grown on fructose (upper panel). The growth curve of the Δ*fruR* with chromosomal duplication of the wild-type *fruR-fruBKA* intergenic region (Δ*fruR*-dupe) at *fruR*-side served as a control. The growth curve of R-Mut-dupe (green) was compared with that of the WT-dupe (black) and Δ*fruR*-dupe (blue) on fructose. The relative mRNA expression of *fruB* and *fruR* in indicated strains are shown relative to corresponding value of WT-dupe grown on glucose (log_2fold changes). The mean and standard deviation of three measurements are shown.

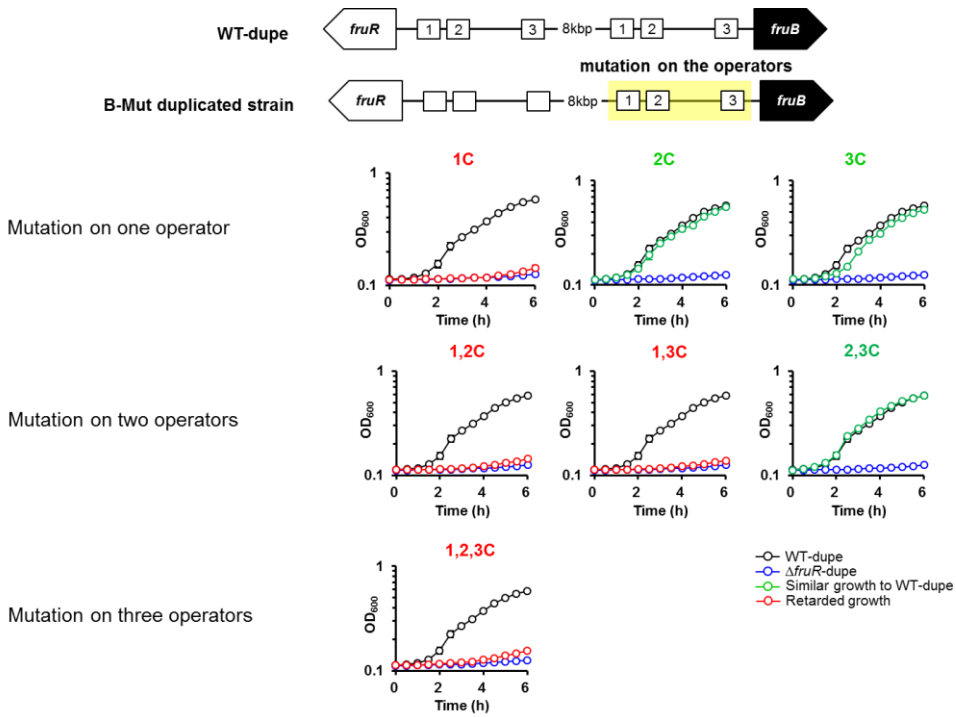

Figure 18. FruR binding to *fruB* O1 is essential for the growth on fructose

V. cholerae strains with chromosomal duplication of the wild-type *fruR-fruBKA* intergenic region (WT-dupe) and duplication of the mutated *fruR-fruBKA* intergenic region at *fruB*-side (B-Mut duplicated strains) were grown on fructose (upper panel). The growth curves of each strain were compared with those of the WT-dupe (black) and Δ*fruR*-dupe (blue) on fructose. Red colors indicate the retarded growth curves and green symbols indicate the growth curves similar to that of the wild type. The mean and standard deviation of three measurements are shown.

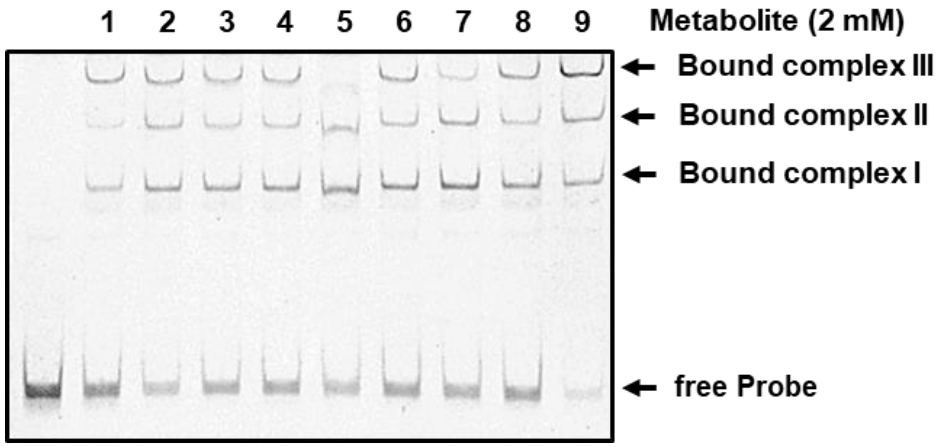

Figure 19. Identification of the metabolite effector of VcFruR

EMSA with VcFruR-DNA mixture containing diverse metabolites was conducted to define the metabolite effector of VcFruR. 60ng of DNA fragments covering entire *fruR-fruBKA* region was incubated with 60 ng of VcFruR and 2 mM of metabolites (lane 2; Glc, lane 3; G6P, lane 4; Fru, lane 5; F1P, lane 6; F6P, lane 7; FBP, lane 8; PEP). Lane 1, 9 contained 45 ng and 90 ng of VcFruR without supplementation of any metabolite.

Our results showed that only treatment with F1P could reduce the cognate band intensity of DNA-FruR complex III.

6.2 F1P releases VcFruR from *fruB* O1 in the FruR-DNA complex.

Since DNA-FruR complex III indicates the VcFruR occupied all three operators, we wondered which operator-FruR complex is to be weakened by the addition of F1P. Previous study has demonstrated that F1P inhibits FruR binding to an operator that contains symmetrical binding sequences in a stronger manner (Ramseier *et al.*, 1993). Since *fruB* O1 consists of a nearly perfect palindromic sequence (Figure 8), we considered that FruR binding to *fruB* O1 may be more sensitive to F1P than other operators. To verify this assumption, a 320-bp probe containing two of three operators (1C, 2C and 3C) were incubated with VcFruR and increasing concentration of F1P. EMSA was performed with these mixtures (Figure 20).

The retarded bands denoting the DNA-FruR complex II disappeared in experiment conducted with only 2C or 3C probe not 1C probe. We reasoned that F1P-mediated release of VcFruR from the DNA mainly occurred at *fruB* O1. To further verify our hypothesis, we measured the binding affinity to each promoter in the absence or presence of 2 mM of F1P. While the binding affinity was not dramatically changed by the addition of F1P in all three operators (data are not shown), F1P reduces the ratio of VcFruR bound form of DNA to unbound form of DNA at the *fruB* O1 (Figure 21).

Footprinting assay with the 320-bp probe containing all three operator sequences also demonstrated that saturated concentration of F1P (2 mM) induces the sequential displacement of VcFruR from each operator (Figure 22). What we found was that VcFruR bound *fruB* O1 showed the most sensitivity to F1P while *fruB* O2 and *fruB* O3 were still protected from DNase I by VcFruR to the extent when the DNA was incubated with half dose of

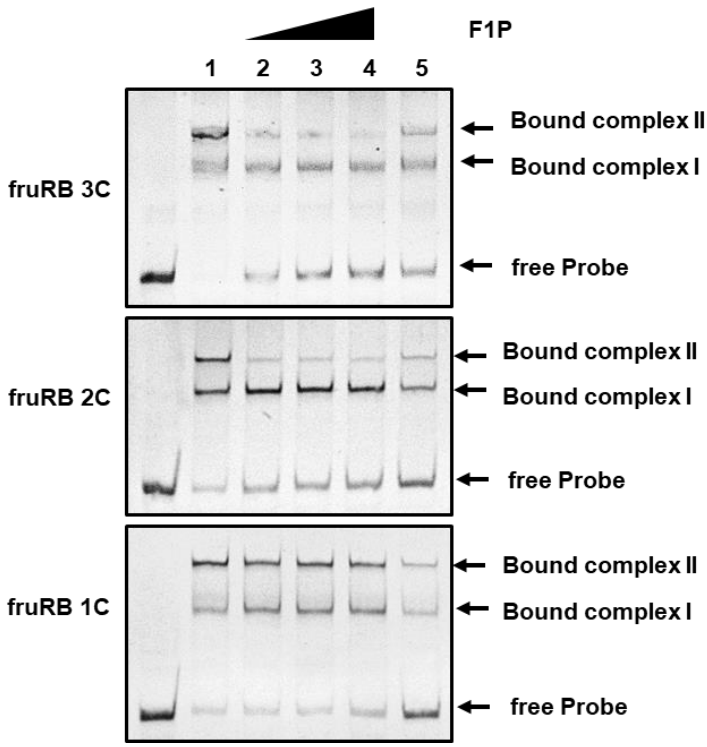

Figure 20. F1P releases VcFruR from the *fruB* O1

DNA fragments containing two of the three operators (1C, 2C and 3C) were incubated with 60 ng of VcFruR in the absence or presence of increasing concentration of F1P. Lane 1-4 contained 60 ng of VcFruR with supplementation of 0.5, 1 and 2 mM of F1P, respectively. Lane 5 contained 30 ng of VcFruR without supplementation of F1P.

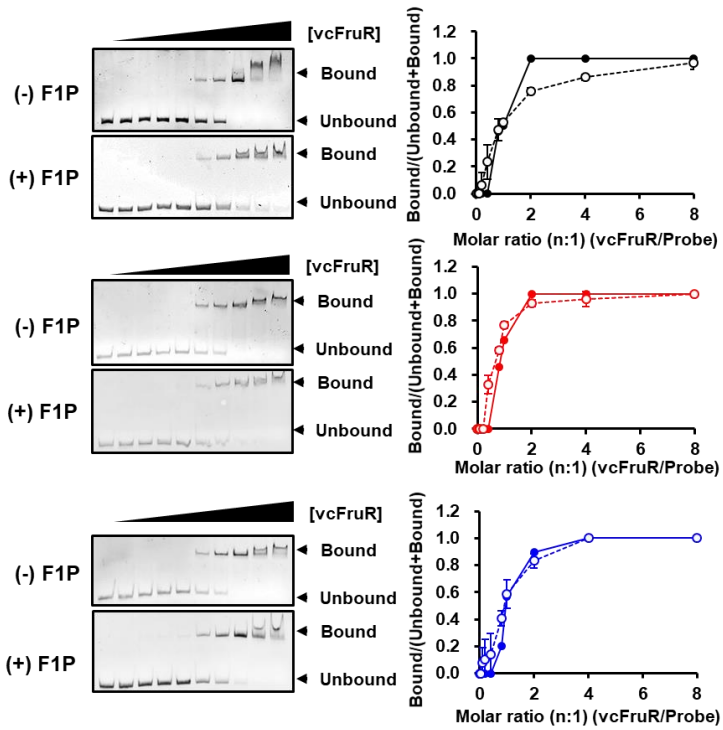

Figure 21. F1P specifically weakens the VcFruR binding to *fruB* O1

Sixty nanogram of the DNA fragments containing one of the operators (Black; *fruB* O1, Red; *fruB* O2, Blue; *fruB* O3) were incubated with increasing amount of VcFruR (0-240 ng). The band intensities of the VcFruR-DNA complex bands (Bound) and free probes (Unbound) were measured in all EMSA conducted with (+ F1P) or without (- F1P) supplementation of 2 mM of F1P (left panel). The band intensity of VcFruR-DNA complexes relative to those of free probe (Bound/Unbound+Bound) was plotted against the molar ratio of VcFruR to probe (n:1) (right panel). Open circles with dotted lines denote the values observed from the experiment conducted with supplementation of F1P and the closed circles with solid lines denote the values observed from the experiment conducted without supplementation of F1P. The mean and standard deviation of three measurements are shown.

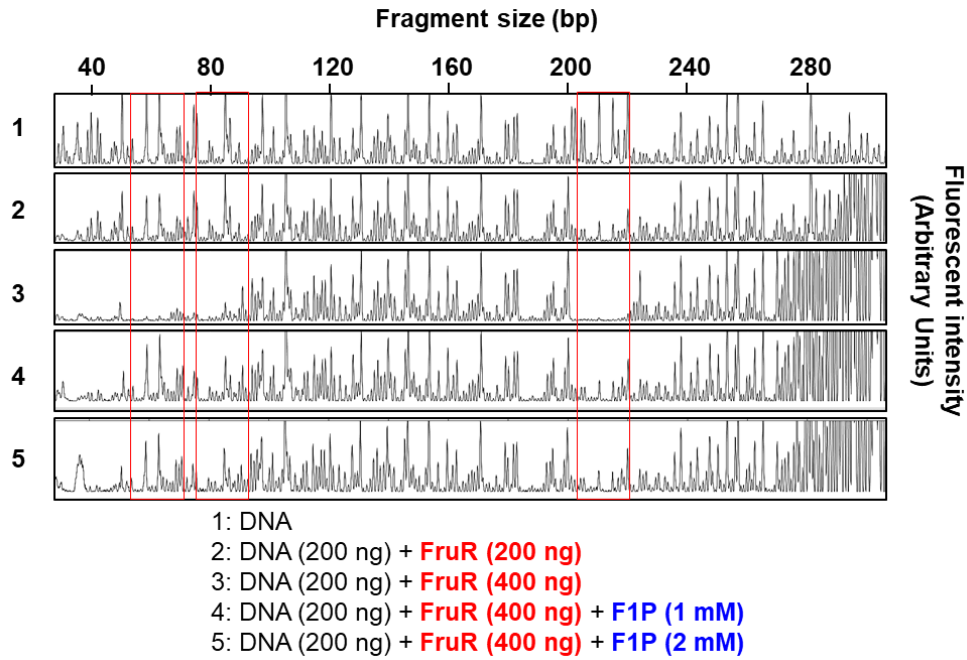

Figure 22. Mapping the VcFruR binding sites sensitive to F1P

To figure out the F1P effect on the VcFruR binding to each operators, DNase1 footprinting assay was conducted with supplementation of F1P. 200 ng of DNA fragments covering entire *fruR-fruBKA* intergenic region was incubated with indicated amount of VcFruR and F1P prior to DNase I digestion. Lane 1-3 contained increasing amount of VcFruR (100 ng, 200 ng and 400 ng, respectively). Lane 4, 5 contained 400 ng of VcFruR supplemented with 1 mM and 2 mM of F1P, respectively. The DNA regions corresponding to *fruB* O1, O2 and O3 which is protected from DNase 1 digestion by VcFruR are marked with red lines. The electropherograms of fluorescent peaks were aligned with manually generated sequence using GeneMapper software (Applied Biosystem).

VcFruR in the absence of F1P (compare the indicated peaks in panel 2 and 5).

6.3 Direct binding of F1P is essential for the activity of VcFruR

Structural, biochemical and biophysical studies have revealed that among the fructose-derived metabolite, F1P is the preferred metabolite effector of FruR ortholog in *P. putida* (PpFruR; 74% similarity and 48% identity with the EcFruR, 64% similarity and 46% identity with VcFruR)(Chavarria *et al.*, 2014). The cavity where F1P molecules interact with PpFruR was determined to be involved with 10 amino acid residues and these amino acid sequences were also conserved in VcFruR. By superimposing the crystal structure of VcFruR with that of PpFruR-F1P complex, we identified that Asn-73 and Arg-197 residues are mainly responsible for the direct binding of F1P (Figure 23). While the protein with the R197A, M and E mutation were insoluble, N73D mutant was soluble and thus was purified for EMSA. EMSA demonstrated that N73D mutant of VcFruR was insensitive to 2 mM of F1P (Figure 24). A *fruR* deletion strain with complementary plasmid carrying the N73D or R197E mutants of VcFruR showed similar growth pattern compared to a *fruR* mutant carrying the empty vector in the fructose medium (Figure 25).

7. The plausible effect of VcFruR-F1P complex on the RNA polymerase in binding to DNA

7.1 VcFruR-mediated activation of the transcription of the *fruBKA* operon requires the intracellular F1P

To investigate the activation mechanism of VcFruR, we examined whether the overexpression of VcFruR without F1P activates the transcription of the *fruBKA* operon. We found that, in the absence of intracellular F1P, overexpressed VcFruR cannot activate the transcription of the *fruBKA* operon

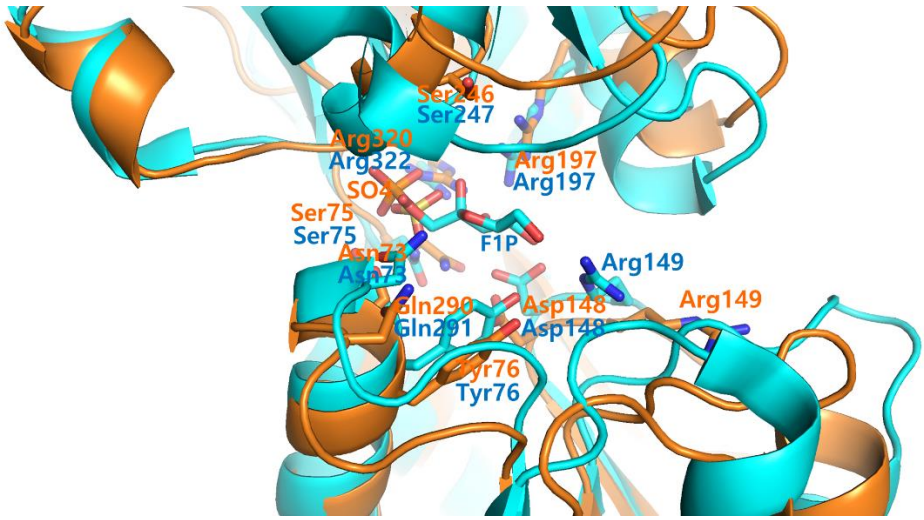

Figure 23. Expected binding modes of F1P with VcFruR.

Crystal structure of VcFruR (coloured in orange) was superimposed onto that of PpFruR (coloured in cyan) in complex with F1P. Overall structures of VcFruR and PpFruR were well matched with the r.m.s.d. of 2.373 Å. A sulfate ion from the crystallization condition was occupied in the putative F1P binding site of VcFruR with the average B-factor of 30.00 $Å^2$. The binding mode of the phosphate moiety of F1P in PpFruR structure was compatible with the binding of sulfate ion in VcFruR, which can suggest the exact binding mode of F1P in VcFruR.

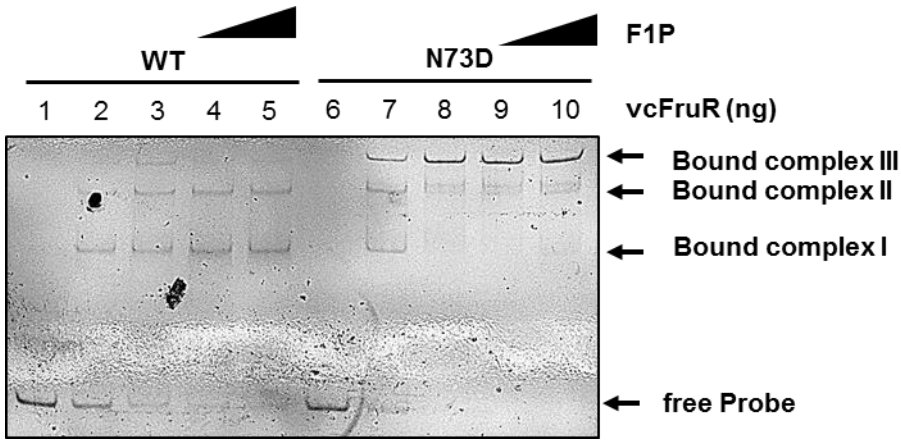

Figure 24. N73D mutant of VcFruR is insensitive to F1P.

EMSA with increasing amount of wild-type VcFruR (WT) (Lane 1-5) or N73D mutant VcFruR (N73D) (Lane 6-10) in the absence or presence of F1P. Lane 1,6 contained no proteins, Lane 2,7 contained 60 ng of VcFruRs without supplementation of F1P, Lane 3,8 contained 120 ng of VcFruRs without supplementation of F1P, Lane 4,9 contained 120 ng of VcFruRs with supplementation of 1 mM of F1P, Lane 5,10 contained 120 ng of VcFruR with supplementation of 2 mM of F1P

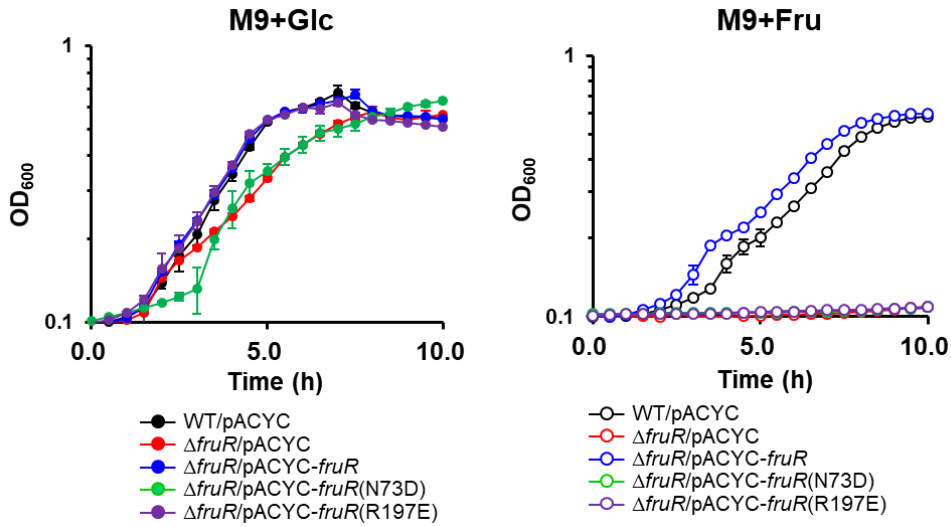

Figure 25. N73D or R197E mutant of VcFruR have no transcriptional regulatory activity

Growth curves of the *fruR* mutants complemented with plasmid carrying the wild-type and mutant of FruR in M9 medium supplemented with 0.2% glucose (left panel) or fructose (right panel) are shown. Black; WT/pACYC, Red; Δ*fruR*/pACYC, Blue; Δ*fruR*/pACYC-*fruR*, Green; Δ*fruR*/pACYC-*fruR*(N73D), Purple; Δ*fruR*/pACYC-*fruR*(R197E)

operon in the wild-type (Figure 26A) and the promoter activity of the plasmid carrying *lacZ* construct in the Δ*fruR* strain (Figure 26B).

7.2 Interaction between VcFruR and RNA polymerase complex on a binding to DNA

We speculated that the VcFruR-F1P complex might interact with RNA polymerase subunits near the *fruB* O1 which results in the transcription activation of the *fruBKA* operon. To investigate the interaction of VcFruR and the RNA polymerase subunits, EMSA was performed with the mixture containing different combination of VcFruR, *E. coli* Core enzyme (ecCore), Sigma 70 of *V. cholerae* (vcσ70) and F1P. A ecCore forms two complexes with DNA (Figure 27, lane 2). The intensities of two ecCore-DNA bands increased with the addition of vcσ70 which possibly resulted in forming a holoenzyme (Figure 27, lane 4). It is reported that among these two bands, a band more distant from the free probe on a gel denotes the open complexes of RNA polymerase (RP_o) and the other band proximal to the free probe denotes the closed complex (RP_c) or intermediate complex (RP_i) (Tupin *et al.*, 2010). Interestingly, the addition of VcFruR increases the RP_o complex band, while decreasing the RP_c complex band (lane 7). To map out the DNA regions occupied with complexes identified in EMSA, footprinting assays were performed under the same condition (Figure 28). We used the probe DNA containing the extended *fruR-fruBKA* intergenic region covering 100 bp downstream of the each start codon of *fruB* and *fruR*. RNApol complex (ecCore+vcσ70) protected about 70-bp DNA region corresponding to 184~114-bp upstream of the TSS, covering the entire *fruB* O1. VcFruR binding induces hyposensitivity to DNase 1 which may be resulting from the DNA bending.

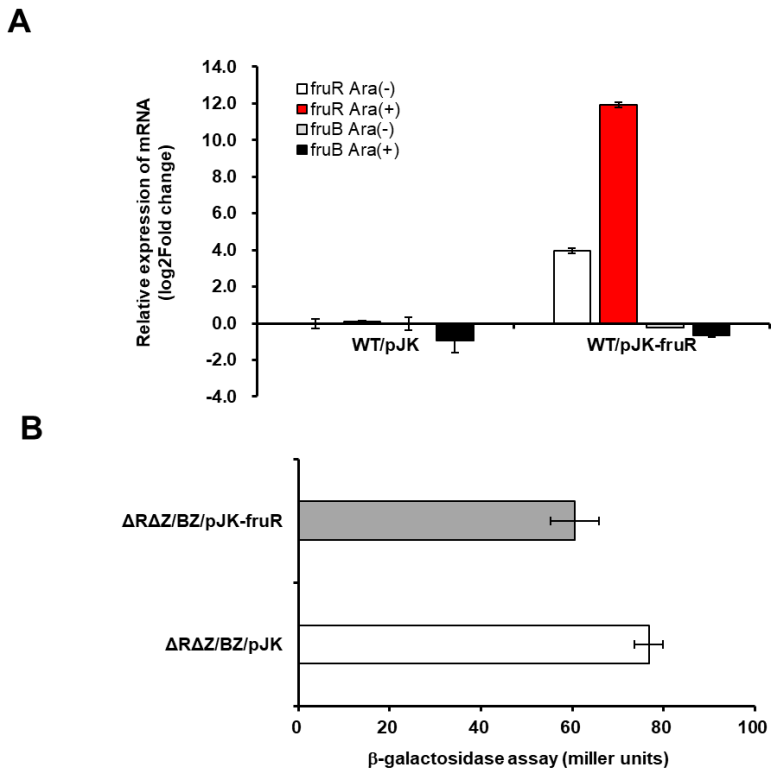

Figure 26. VcFruR cannot activate the transcription of the *fruBKA* operon in the absence of F1P

(A) Plasmid-borne expression of VcFruR cannot induces the *fruBKA* mRNA expression in the absence of F1P. Wild type N16961 were transformed with empty vector (WT/pJK) or VcFruR-expression vector (WT/pJK-*fruR*). Two strains were cultured at LB medium supplemented with (+) or without (-) 0.2% arabinose until OD reaches 0.5. The relative mRNA expression of *fruR* and *fruB* were measured and compared to the corresponding value obtained from WT/pJK cultured at Ara(-) medium **(B)** In the absence of F1P, the overexpression of VcFruR cannot induces the *fruBKA* promoter. β-galactosidase assays using the Δ*fruR*Δ*lacZ*/BZ strain transformed with pJK-*fruR* was conducted. Two strains were cultured at LB medium supplemented with 0.2% arabinose.

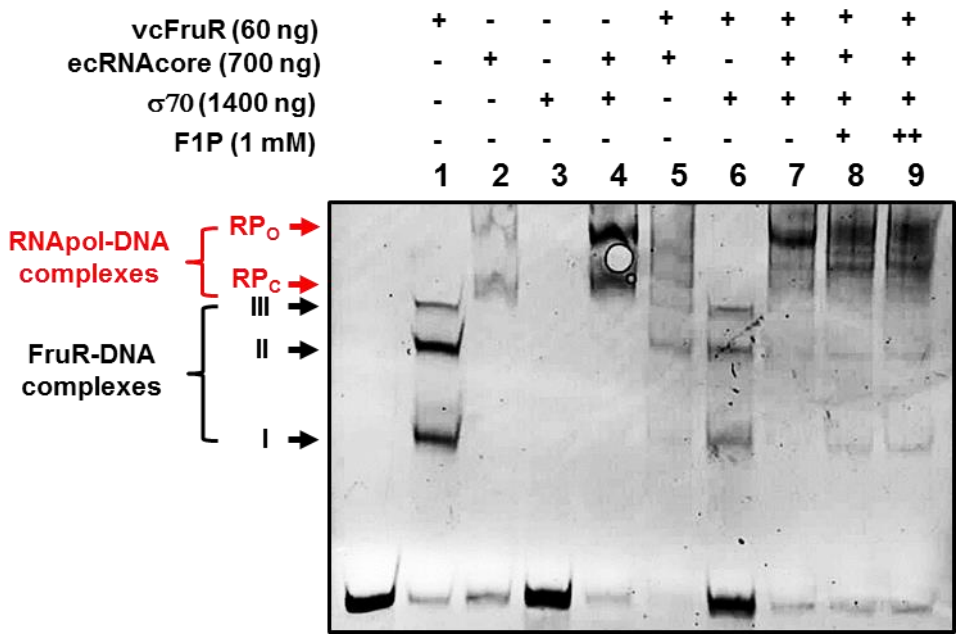

Figure 27. Dynamic interaction of VcFruR and RNA polymerase complex

EMSA with VcFruR, *E. coli* core enzyme of RNA polymerase (EcCore) and *V. cholerae* Sigma factor 70 (Vcσ70) was conducted in the absence or presence of 2 mM of F1P. "+" and "-" symbols represent the presence or absence of the proteins or chemicals as indicated on the left. Each DNA-RNApol complexes and DNA-VcFruR complexes are marked with red and black arrows on the left. RP_o; open complexes of RNA polymerase RP_c; closed complex of RNA polymerase

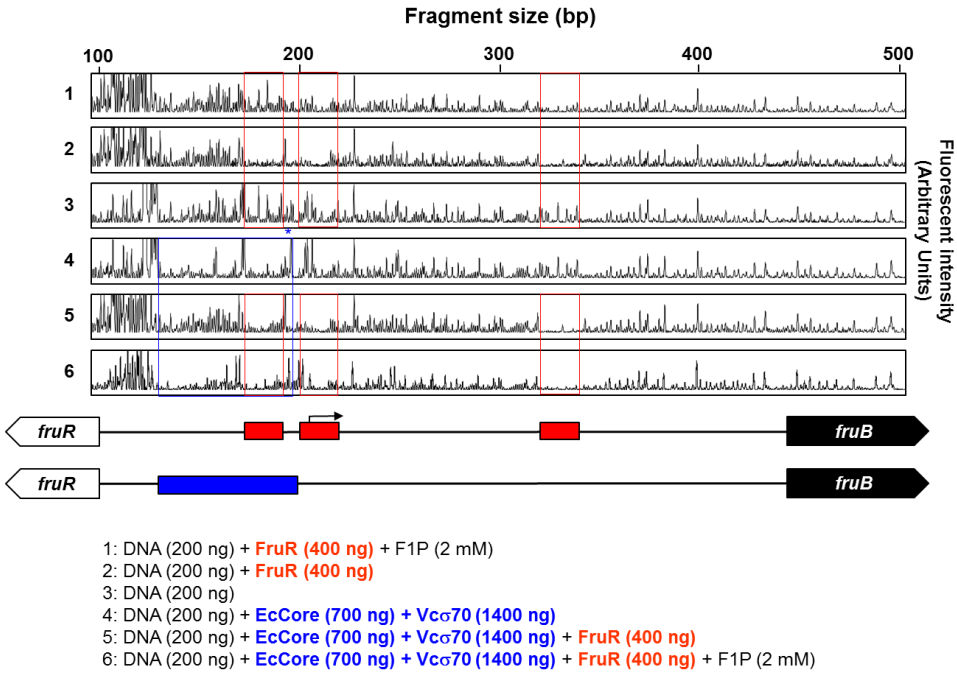

1: DNA (200 ng) + **FruR (400 ng)** + F1P (2 mM)
2: DNA (200 ng) + **FruR (400 ng)**
3: DNA (200 ng)
4: DNA (200 ng) + **EcCore (700 ng) + Vcσ70 (1400 ng)**
5: DNA (200 ng) + **EcCore (700 ng) + Vcσ70 (1400 ng)** + **FruR (400 ng)**
6: DNA (200 ng) + **EcCore (700 ng) + Vcσ70 (1400 ng)** + **FruR (400 ng)** + F1P (2 mM)

Figure 28. The effect of F1P on the interaction between VcFruR and RNA polymerase in binding to DNA.

A 200 ng of 6-FAM-labelled DNA fragment containing extended *fruR-fruBKA* intergenic region was incubated with different combination of proteins and F1P. The regions protected from DNase 1 digestion by RNApol complex (blue line) were compared with regions protected from DNase 1 digestion by VcFruR (red line). Red and blue boxes indicate the VcFruR-mediated and RNApol complex-mediated protected DNA regions from DNase I digestion (lower panel). Curved arrow indicates the TSS of the *fruBKA* operon.

induced by VcFruR. However, binding of RNApol complex induces hypersensitivity to DNase1 at the same DNA region (Figure 28, blue asterisks). Interestingly, when the RNApol complexes competed with VcFruR, VcFruR interrupted the binding of RNA polymerase to the DNA region upstream of *fruB* O1.

Chapter IV. Discussion

1. Non-canonical mechanism of transcriptional activation by VcFruR

In this study, we proposed a non-canonical mechanism of VcFruR-mediated transcriptional activation (Figure 29). In the presence of F1P, VcFruR activates the transcription of the *fruBKA* through binding to the operator located between -35 and -10 region of the promoter. F1P alters the mode of VcFruR binding to this operator which facilitates the binding of RNA polymerase complex to the promoter.

1.1 The canonical mechanism of transcriptional regulation by FruR

The canonical mechanism of transcriptional regulation by FruR has been established based on the experimental evidences conducted with FruR orthologs of the species belonging to *Enterobacteriaceae* (*E. coli*) and *Pseudomonadaceae* (*P. putida*) (Figure 29). In *E. coli*, FruR binds to two operators located respectively at 7.5-bp and 73.5-bp downstream relative to the TSS and the genomic loci of *fruR* is distant from the *fruBKA* operon. In *P. putida*, FruR binds to one operator located 19.5-bp downstream of the TSS of the *fruBKA* (Chavarria *et al.*, 2011). Unlike in *E. coli*, in *P. putida*, the genomic arrangement of *fruR* is also divergently oriented and transcribed from the *fruBKA* operon as in *V. cholerae*. Despite the different genomic distribution of *fruR* and the *fruBKA* operon between two species, a *fruR* mutant exhibited increase in the uptake rate of fructose (Yao *et al.*, 2013) and overexpression of *fruBKA* mRNA expression (Chavarria *et al.*, 2011) than the wild type in both species. *V. cholerae* also has an operator located downstream of the TSS but binding on this operator has little effect on the transcriptional regulation of the *fruBKA* operon. However, the F1P-sensitive binding at *fruB* O1 determines the activation of the transcription of the *fruBKA* operon, which implies that canonical mechanism of transcriptional regulation by FruR has to be complemented with many other experiments.

A

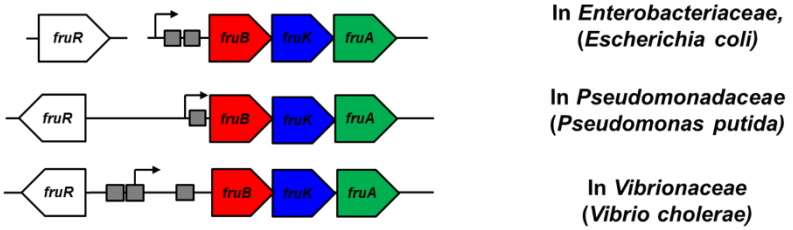

B

		Enterobacteriaceae, Pseudomonadaceae	*Vibrionaceae*
Characteristics of FruR	Oligomeric state of FruR	Tetramer or Dimer	Dimer
	Metabolite effector	F1P	F1P
Mode of transcriptional regulation		Repressor	**Activator**
Binding site	Number of operator(s)	2 or 1	**3**
	Orientation and distance from the TSS	downstream of	**one operator contains TSS one operator downstream and one operator upstream of**
Effects of *fruR* deletion	Transcription of the *fruBKA* operon	Increases	**No transcription**
	Growth rate on fructose	Enhanced growth	Retarded growth

Figure 29. The comparison between canonical and non-canonical transcriptional regulation of the *fruBKA* operon by FruR in *Gammaproteobacteria*.

(A) The schematics of the genomic distribution of *fruR* and the *fruBKA* operon in the three different species (*E. coli*, *P. putida* and *V. cholerae*) which belong to the *Gammaproteobacteria*. The *fruR* ORF and *fruB* ORF are indicated with white and red boxes, respectively. The gray boxes represent the FruR-binding sites and curved arrows indicate the TSSs of the *fruBKA* operons. (B) The comparison of traits between canonical and non-canonical transcriptional regulation of the *fruBKA* operon by FruR. FruR orthlogs in species of *Enterobacteriaceae* and *Pseudomonadaceae* act as a canonical transcription repressor. However, in *V. cholerae*, FruR acts as a non-canonical transcriptional activator.

1.2. FruR acts as a transcription activator of other target genes

Previous works demonstated that EcFruR acts as a transcription activator of *ppsA*, *icdE*, *pckA* and *aceBAK* operon (Negre *et al.*, 1998, Prost *et al.*, 1999). EcFruR binding sites are located at the 45.5 bp (*ppsA*), 76.5 bp (*icdE*), 145.5 bp (*pckA*) and 170.5 bp (*aceBAK*) upstream of the TSSs of target genes (Ramseier *et al.*, 1995). Other studies suggested the mechanism of EcFruR as a transcription activator which binds to multiple operators (Reshamwala & Noronha, 2011). Authors identified three EcFruR-binding sites in the *csgDEFG* promoter region, which located at 46-bp downstream (O1) of and 202-bp, 233-bp upstream (O2, O3) of the TSS of the operon. While all three operators are required for maximal transcription, the O1 operator plays a major role, as mutation in this region led to a 70% reduction of mRNA expression. However, proposed mechanism in this study is completely different from our suggestion in that VcFruR bound on the operator located most distant upstream of TSS has essential roles in the activation of transcription. Another study demonstrated that two EcFruR-binding sites are centered at 105.5-bp and 134.5-bp upstream of the TSS of the *cydAB* operon which encodes subunit I and II of cytochrome bd-I terminal oxidase. Authors assumed that EcFruR acts as a transcription activator of the operon. However, no experimental evidence was demonstrated based on the hypothesis (Ramseier, 1996)

2. Novel features of the non-canonical regulation of VcFruR

2.1. VcFruR appears to be the member of MerR-type transcriptional activators

It has been known that by directly binding to both target DNA and the component(s) of RNA polymerase, transcription factor activates the promoter and improves its affinity for RNA polymerase. The three general binding

mechanisms of transcriptional activators have been known; transcription factors bind to the DNA upstream of -35 element interacting with the RNA polymerase α subunit C-terminal domain (Class I) or -35 element interacting with sigma subunit domain 4 (Class II) or between -10 and -35 element altering the conformation of a promoter (MerR type) (Browning & Busby, 2004). Since the position of *fruB* O1, the essential binding site of VcFruR for the transcriptional activation of the *fruBKA* operon, is between -10 and -35 region, VcFruR appears to be a MerR-type transcription regulator. The following properties of VcFruR-mediated transcriptional regulation also support that VcFruR belongs to the MerR family of transcriptional regulators: First, as MerR acts as transcription activator only in the presence of an effector (Hg(II)), VcFruR activates the transcription of the *fruBKA* operon only in the presence of the effector F1P. Second, as RNA polymerase binding region overlaps with the *fruB* O1 (Figure 28), MerR and RNA polymerase bind to the promoter simultaneously (O'Halloran *et al.*, 1989). Third, the divergent genomic arrangement of the *fruR* and the *fruBKA* operon is similar to that of the *merR* and the major regulated *merTP(C/F)AD(E)* operon (*mer* operon). Fourth, VcFruR forms a homodimer (Figure 7), as do all MerR-type members of transcription regulators (Brown *et al.*, 2003). In the absence of F1P, it was confirmed that VcFruR bound to *fruB* O1 slightly interfered with the RNA polymerase binding to the promoter region (Figure 28) and that VcFruR exhibits no transcriptional activation (Figure 26). However, in the presence of F1P, VcFruR-F1P complex activates the transcription of the *fruBKA* operon. In the case of MerR, in the absence of Hg(II), the MerR is bound to the DNA in the repressor conformation maintaining transcriptional repression of the promoter. However, in the presence of Hg(II), MerR binds to the promoter region between -10 and -35 to distort the DNA structure and allow RNA polymerase to form an open initiation complexes. Consequently,

we assumed that VcFruR also enhances the binding of RNA polymerase to the promoter in a manner similar to MerR-mediated transcriptional activation.

2.2. Multiple binding of FruR on a promoter region

Among the 1303 LacI-TFs in 272 bacterial genome, only 116 operons (~2% of regulated operons) are regulated by three adjacent sites. However, by analyzing the datasets of SELEX experiment and ChIP with Exonuclease treatment (ChIP-exo) experiment, we found that multiple binding to more than one operator of FruR only occured at the promoter region of the *fruBKA* operon in *E. coli* (Shimada *et al.*, 2011, Kim *et al.*, 2018). Shimada *et al.*, discussed that the putative binding site centered at 273.5-bp upstream of the TSS of *setB*, which is divergently transcribed from the *fruB*, might be the 3rd operator of *fruB*. However, the researchers were confused with the distance from the *setB* operator to TSS of *fruB* with the distance from the *setB* operator to start codon of *fruB*. Thus, the operator, which lies in *setB* promoter region, is the first operator of *fruB*. Hence, to our best knowledge, there has been no report that the promoter region of FruR target gene(s) possesses triple binding sites. Our studies shows that *fruB* O1 and O2 lie in close proximity to *fruR* ORF and is separated with 6-bp long DNA sequences. A *fruB* O3 is located at 111-bp downstream of the *fruB* O2. The distances between the centers of O1 and O2 (22 bp), O2 and O3 (127 bp) approximately equal the multiples of DNA helical turn (10.5 bp), which implies cooperative binding of transcription factor can occur (Dunn *et al.*, 1984).

3. FruR is not a global transcription regulator

Being a direct repressor of *fruBKA* operon ever since it was discovered, FruR has been investigated as a global transcription regulator based on the incorrect experimental data that FBP reduces its binding affinity to the FruR operators

in approximately 160 promoters. Two recent works examined and confirmed the global regulatory effect of FruR in two species belonging to *Gammaproteobacteria*, *E. coli* and *P. putida*. However, the data demonstrated in these studies cast doubt on whether FruR indeed acts as a global regulator or not.

In *E. coli*, 49 putative FruR-binding sites and 97 genes as a FruR regulon were identified with ChIP-exo experiment and mRNA sequencing experiment, respectively (Kim *et al.*, 2018). However, these two data were not that relevant to each other. Among the 49 binding site, EcFruR binding dependent on the sugar source (i.e, occurs on glucose and acetate medium but not occurs on fructose medium or vice versa) occurs only at 20 binding sites. Suprisingly, furthermore, EcFruR bound on a *fruBKA* promoter occurs in cell cultured in all three different carbon source. However, among these genes, mRNA expression of only six genes were changed by the existence of EcFruR in fructose medium, which means that most of these genes are not the EcFruR regulon. For the precise analysis, we re-analyzed the FPKM ratio of WT-fru versus WT-glu, ratio of Δ*fruR*-fru versus Δ*fruR* -glu and ratio of Δ*fruR*-fru versus WT-fru. Among the genes whose promoter has putative EcFruR binding operators, only *fruBKA* genes showed appropriate value and other 48 genes that has putative EcFruR binding site are not on the list (data are not shown). These imply that EcFruR has minimal effect on the expression of metabolic genes other than *fruBKA* and EcFruR-mediated regulation is dependent on the extent of EcFruR binding rather than the occurrence of EcFruR binding.

In *P. putida*, genome-wide mRNA sequencing unraveled the other target gene of PpFruR, which is one of the glycerol-3-phosphate dehydrogenase (GAPDH) enzyme (Chavarria *et al.*, 2016). Authors suggest that by changing the expression or activity of GAPDH, *P. putida* can alter the metabolic flux.

However, there are no detailed molecular experiment proving the fact such as PpFruR binds to GAPDH promoter or the presence of the F1P affect the expression of GAPDH mRNA. We conducted similar experiment performed in those two studies, searching for binding sites based on the known consensus sequences (Table 4). RNA sequencing was performed to examine the direct sugar effect on the global transcriptome (Table 3). We finally discovered that among 40 putative VcFruR binding sites located in the *V. cholerae* chromosomes, VcFruR only binds to and regulates four genes. As most of the metabolic genes are modulated by cooperative performance of multiple transcription factors, these experimental data suggesting the global roles of FruR do not unravel the precise FruR mechanism. In summary, we assumed that FruR mainly acts as a fructose regulator, not a metabolic regulator in at least three bacterial species.

Chapter V. References

Barabote, R.D., and Saier, M.H., Jr. (2005) Comparative genomic analyses of the bacterial phosphotransferase system. *Microbiol Mol Biol Rev* **69**: 608-634.

Bennett, B.D., Kimball, E.H., Gao, M., Osterhout, R., Van Dien, S.J., and Rabinowitz, J.D. (2009) Absolute metabolite concentrations and implied enzyme active site occupancy in *Escherichia coli*. *Nat Chem Biol* **5**: 593-599.

Bledig, S.A., Ramseier, T.M., and Saier, M.H., Jr. (1996) Frur mediates catabolite activation of pyruvate kinase (*pykF*) gene expression in *Escherichia coli*. *J Bacteriol* **178**: 280-283.

Bley Folly, B., Ortega, A.D., Hubmann, G., Bonsing-Vedelaar, S., Wijma, H.J., van der Meulen, P., Milias-Argeitis, A., and Heinemann, M. (2018) Assessment of the interaction between the flux-signaling metabolite fructose-1,6-bisphosphate and the bacterial transcription factors CggR and Cra. *Mol Microbiol* **109**: 278-290.

Brown, N.L., Stoyanov, J.V., Kidd, S.P., and Hobman, J.L. (2003) The MerR family of transcriptional regulators. *FEMS microbiology reviews* **27**: 145-163.

Browning, D.F., and Busby, S.J. (2004) The regulation of bacterial transcription initiation. *Nat Rev Microbiol* **2**: 57-65.

Buescher, J.M., Moco, S., Sauer, U., and Zamboni, N. (2010) Ultrahigh performance liquid chromatography-tandem mass spectrometry method for fast and robust quantification of anionic and aromatic metabolites. *Anal Chem* **82**: 4403-4412.

Chang, A.C., and Cohen, S.N. (1978) Construction and characterization of amplifiable multicopy DNA cloning vehicles derived from the P15A cryptic miniplasmid. *J Bacteriol* **134**: 1141-1156.

Chavarria, M., Durante-Rodriguez, G., Krell, T., Santiago, C., Brezovsky, J.,

Damborsky, J., and de Lorenzo, V. (2014) Fructose 1-phosphate is the one and only physiological effector of the Cra (FruR) regulator of *Pseudomonas putida*. *FEBS Open Bio* **4**: 377-386.

Chavarria, M., Fuhrer, T., Sauer, U., Pfluger-Grau, K., and de Lorenzo, V. (2013) Cra regulates the cross-talk between the two branches of the phosphoenolpyruvate : phosphotransferase system of *Pseudomonas putida*. *Environ Microbiol* **15**: 121-132.

Chavarria, M., Goni-Moreno, A., de Lorenzo, V., and Nikel, P.I. (2016) A Metabolic Widget Adjusts the Phosphoenolpyruvate-Dependent Fructose Influx in *Pseudomonas putida*. *mSystems* **1**.

Chavarria, M., Santiago, C., Platero, R., Krell, T., Casasnovas, J.M., and de Lorenzo, V. (2011) Fructose 1-phosphate is the preferred effector of the metabolic regulator Cra of *Pseudomonas putida*. *J Biol Chem* **286**: 9351-9359.

Choi, S.H., Lee, K.L., Shin, J.H., Cho, Y.B., Cha, S.S., and Roe, J.H. (2017) Zinc-dependent regulation of zinc import and export genes by Zur. *Nat Commun* **8**: 15812.

Cortay, J.C., Negre, D., Scarabel, M., Ramseier, T.M., Vartak, N.B., Reizer, J., Saier, M.H., Jr., and Cozzone, A.J. (1994) *In vitro* asymmetric binding of the pleiotropic regulatory protein, FruR, to the *ace* operator controlling glyoxylate shunt enzyme synthesis. *J Biol Chem* **269**: 14885-14891.

Crasnier-Mednansky, M., Park, M.C., Studley, W.K., and Saier, M.H., Jr. (1997) Cra-mediated regulation of *Escherichia coli* adenylate cyclase. *Microbiology* **143 (Pt 3)**: 785-792.

Dunn, T.M., Hahn, S., Ogden, S., and Schleif, R.F. (1984) An operator at-280 base pairs that is required for repression of *araBAD* operon promoter: addition of DNA helical turns between the operator and promoter

cyclically hinders repression. *Proceedings of the National Academy of Sciences* **81**: 5017-5020.

Feldheim, D.A., Chin, A.M., Nierva, C.T., Feucht, B.U., Cao, Y.W., Xu, Y.F., Sutrina, S.L., and Saier, M.H., Jr. (1990) Physiological consequences of the complete loss of phosphoryl-transfer proteins HPr and FPr of the phosphoenolpyruvate:sugar phosphotransferase system and analysis of fructose (*fru*) operon expression in *Salmonella typhimurium*. *J Bacteriol* **172**: 5459-5469.

Ferenci, T., and Kornberg, H.L. (1974) The role of phosphotransferase-mediated syntheses of fructose 1-phosphate and fructose 6-phosphate in the growth of *Escherichia coli* on fructose. *Proceedings of the Royal Society of London. Series B. Biological Sciences* **187**: 105-119.

Grisafi, P.L., Scholle, A., Sugiyama, J., Briggs, C., Jacobson, G.R., and Lengeler, J.W. (1989) Deletion mutants of the *Escherichia coli* K-12 mannitol permease: dissection of transport-phosphorylation, phospho-exchange, and mannitol-binding activities. *J Bacteriol* **171**: 2719-2727.

Gupta, K.D., and Ghosh, S. (1984) Identification of a phosphoenolpyruvate:fructose 1-phosphotransferase system in *Azospirillum brasilense*. *J Bacteriol* **160**: 1204-1206.

Hamashima, H., Iwasaki, M., and Arai, T. (1995) A simple and rapid method for transformation of *Vibrio* species by electroporation. *Methods Mol Biol* **47**: 155-160.

Hayes, C.A., Dalia, T.N., and Dalia, A.B. (2017) Systematic genetic dissection of PTS in *Vibrio cholerae* uncovers a novel glucose transporter and a limited role for PTS during infection of a mammalian host. *Mol Microbiol* **104**: 568-579.

Houot, L., Chang, S., Absalon, C., and Watnick, P.I. (2010a) *Vibrio cholerae*

phosphoenolpyruvate phosphotransferase system control of carbohydrate transport, biofilm formation, and colonization of the germfree mouse intestine. *Infect Immun* **78**: 1482-1494.

Houot, L., Chang, S., Pickering, B.S., Absalon, C., and Watnick, P.I. (2010b) The phosphoenolpyruvate phosphotransferase system regulates *Vibrio cholerae* biofilm formation through multiple independent pathways. *J Bacteriol* **192**: 3055-3067.

Houot, L., and Watnick, P.I. (2008) A novel role for enzyme I of the V*ibrio cholerae* phosphoenolpyruvate phosphotransferase system in regulation of growth in a biofilm. *J Bacteriol* **190**: 311-320.

Jang, K.K., Lee, Z.W., Kim, B., Jung, Y.H., Han, H.J., Kim, M.H., Kim, B.S., and Choi, S.H. (2017) Identification and characterization of *Vibrio vulnificus* plpA encoding a phospholipase A2 essential for pathogenesis. *J Biol Chem* **292**: 17129-17143.

Kim, D., Seo, S.W., Gao, Y., Nam, H., Guzman, G.I., Cho, B.K., and Palsson, B.O. (2018) Systems assessment of transcriptional regulation on central carbon metabolism by Cra and CRP. *Nucleic Acids Res* **46**: 2901-2917.

Kim, H.M., Park, Y.H., Yoon, C.K., and Seok, Y.J. (2015) Histidine phosphocarrier protein regulates pyruvate kinase A activity in response to glucose in *Vibrio vulnificus*. *Mol Microbiol* **96**: 293-305.

Kochanowski, K., Gerosa, L., Brunner, S.F., Christodoulou, D., Nikolaev, Y.V., and Sauer, U. (2017) Few regulatory metabolites coordinate expression of central metabolic genes in *Escherichia coli*. *Mol Syst Biol* **13**: 903.

Kornberg, H.L. (2001) Routes for fructose utilization by *Escherichia coli*. *J Mol Microbiol Biotechnol* **3**: 355-359.

Kundig, W., Ghosh, S., and Roseman, S. (1964) Phosphate Bound to Histidine

in a Protein as an Intermediate in a Novel Phospho-Transferase System. *Proc Natl Acad Sci U S A* **52**: 1067-1074.

Lee, J.W., Park, Y.H., and Seok, Y.J. (2018) Rsd balances (p)ppGpp level by stimulating the hydrolase activity of SpoT during carbon source downshift in *Escherichia coli*. *Proc Natl Acad Sci U S A* **115**: E6845-E6854.

Lessie, T.G., and Phibbs, P.V., Jr. (1984) Alternative pathways of carbohydrate utilization in pseudomonads. *Annu Rev Microbiol* **38**: 359-388.

Lim, J.G., Bang, Y.J., and Choi, S.H. (2014) Characterization of the *Vibrio vulnificus* 1-Cys peroxiredoxin Prx3 and regulation of its expression by the Fe-S cluster regulator IscR in response to oxidative stress and iron starvation. *J Biol Chem* **289**: 36263-36274.

Livny, J., Zhou, X., Mandlik, A., Hubbard, T., Davis, B.M., and Waldor, M.K. (2014) Comparative RNA-Seq based dissection of the regulatory networks and environmental stimuli underlying *Vibrio parahaemolyticus* gene expression during infection. *Nucleic Acids Res* **42**: 12212-12223.

Mandlik, A., Livny, J., Robins, W.P., Ritchie, J.M., Mekalanos, J.J., and Waldor, M.K. (2011) RNA-Seq-based monitoring of infection-linked changes in *Vibrio cholerae* gene expression. *Cell Host Microbe* **10**: 165-174.

Manneh-Roussel, J., Haycocks, J.R.J., Magan, A., Perez-Soto, N., Voelz, K., Camilli, A., Krachler, A.M., and Grainger, D.C. (2018) cAMP Receptor Protein Controls *Vibrio cholerae* Gene Expression in Response to Host Colonization. *MBio* **9**.

Mikulskis, A., Aristarkhov, A., and Lin, E.C. (1997) Regulation of expression of the ethanol dehydrogenase gene (*adhE*) in *Escherichia coli* by

catabolite repressor activator protein Cra. *J Bacteriol* **179**: 7129-7134.

Miller, V.L., and Mekalanos, J.J. (1988) A novel suicide vector and its use in construction of insertion mutations: osmoregulation of outer membrane proteins and virulence determinants in *Vibrio cholerae* requires toxR. *J Bacteriol* **170**: 2575-2583.

Milton, D.L., O'Toole, R., Horstedt, P., and Wolf-Watz, H. (1996) Flagellin A is essential for the virulence of *Vibrio anguillarum*. *J Bacteriol* **178**: 1310-1319.

Munch, R., Hiller, K., Grote, A., Scheer, M., Klein, J., Schobert, M., and Jahn, D. (2005) Virtual Footprint and PRODORIC: an integrative framework for regulon prediction in prokaryotes. *Bioinformatics* **21**: 4187-4189.

Negre, D., Bonod-Bidaud, C., Geourjon, C., Deleage, G., Cozzone, A.J., and Cortay, J.C. (1996) Definition of a consensus DNA-binding site for the *Escherichia coli* pleiotropic regulatory protein, FruR. *Mol Microbiol* **21**: 257-266.

Negre, D., Oudot, C., Prost, J.F., Murakami, K., Ishihama, A., Cozzone, A.J., and Cortay, J.C. (1998) FruR-mediated transcriptional activation at the *ppsA* promoter of *Escherichia coli*. *J Mol Biol* **276**: 355-365.

O'Halloran, T.V., Frantz, B., Shin, M.K., Ralston, D.M., and Wright, J.G. (1989) The MerR heavy metal receptor mediates positive activation in a topologically novel transcription complex. *Cell* **56**: 119-129.

Oehler, S., Eismann, E.R., Kramer, H., and Muller-Hill, B. (1990) The three operators of the lac operon cooperate in repression. *EMBO J* **9**: 973-979.

Papapanagiotou, I., Streeter, S.D., Cary, P.D., and Kneale, G.G. (2007) DNA structural deformations in the interaction of the controller protein C.AhdI with its operator sequence. *Nucleic Acids Res* **35**: 2643-2650.

Papenfort, K., Forstner, K.U., Cong, J.P., Sharma, C.M., and Bassler, B.L. (2015) Differential RNA-seq of *Vibrio cholerae* identifies the VqmR small RNA as a regulator of biofilm formation. *Proc Natl Acad Sci U S A* **112**: E766-775.

Park, S., Yoon, J., Lee, C.R., Lee, J.Y., Kim, Y.R., Jang, K.S., Lee, K.H., and Seok, Y.J. (2019) Polar landmark protein HubP recruits flagella assembly protein FapA under glucose limitation in *Vibrio vulnificus*. *Mol Microbiol*.

Prost, J.F., Negre, D., Oudot, C., Murakami, K., Ishihama, A., Cozzone, A.J., and Cortay, J.C. (1999) Cra-dependent transcriptional activation of the icd gene of *Escherichia coli*. *J Bacteriol* **181**: 893-898.

Ramseier, T. (1996) Cra and the control of carbon flux via metabolic pathways. *Research in microbiology* **147**: 489-493.

Ramseier, T.M., Bledig, S., Michotey, V., Feghali, R., and Saier, M.H., Jr. (1995) The global regulatory protein FruR modulates the direction of carbon flow in *Escherichia coli*. *Mol Microbiol* **16**: 1157-1169.

Ramseier, T.M., Negre, D., Cortay, J.C., Scarabel, M., Cozzone, A.J., and Saier, M.H., Jr. (1993) *In vitro* binding of the pleiotropic transcriptional regulatory protein, FruR, to the *fru*, *pps*, *ace*, *pts* and icd operons of *Escherichia coli* and *Salmonella typhimurium*. *J Mol Biol* **234**: 28-44.

Ravcheev, D.A., Khoroshkin, M.S., Laikova, O.N., Tsoy, O.V., Sernova, N.V., Petrova, S.A., Rakhmaninova, A.B., Novichkov, P.S., Gelfand, M.S., and Rodionov, D.A. (2014) Comparative genomics and evolution of regulons of the LacI-family transcription factors. *Front Microbiol* **5**: 294.

Reizer, J., Reizer, A., and Saier, M.H., Jr. (1995) Novel phosphotransferase system genes revealed by bacterial genome analysis--a gene cluster

encoding a unique Enzyme I and the proteins of a fructose-like permease system. *Microbiology* **141 (Pt 4)**: 961-971.

Reshamwala, S.M., and Noronha, S.B. (2011) Biofilm formation in Escherichia colicra mutants is impaired due to down-regulation of curli biosynthesis. *Archives of microbiology* **193**: 711.

Rolfes, R.J., and Zalkin, H. (1990) Autoregulation of *Escherichia coli* purR requires two control sites downstream of the promoter. *J Bacteriol* **172**: 5758-5766.

Ryu, S., Ramseier, T.M., Michotey, V., Saier, M.H., Jr., and Garges, S. (1995) Effect of the FruR regulator on transcription of the *pts* operon in *Escherichia coli*. *J Biol Chem* **270**: 2489-2496.

Ryu, Y., Kim, Y.J., Kim, Y.R., and Seok, Y.J. (2012) Expression of *Vibrio vulnificus* insulin-degrading enzyme is regulated by the cAMP-CRP complex. *Microbiology* **158**: 1294-1303.

Saier, M.H., Jr., and Ramseier, T.M. (1996) The catabolite repressor/activator (Cra) protein of enteric bacteria. *J Bacteriol* **178**: 3411-3417.

Sarkar, D., Siddiquee, K.A., Arauzo-Bravo, M.J., Oba, T., and Shimizu, K. (2008) Effect of *cra* gene knockout together with *edd* and *iclR* genes knockout on the metabolism in *Escherichia coli*. *Arch Microbiol* **190**: 559-571.

Shimada, T., Fujita, N., Maeda, M., and Ishihama, A. (2005) Systematic search for the Cra-binding promoters using genomic SELEX system. *Genes Cells* **10**: 907-918.

Shimada, T., Yamamoto, K., and Ishihama, A. (2011) Novel members of the Cra regulon involved in carbon metabolism in *Escherichia coli*. *J Bacteriol* **193**: 649-659.

Siebold, C., Flukiger, K., Beutler, R., and Erni, B. (2001) Carbohydrate transporters of the bacterial phosphoenolpyruvate: sugar

phosphotransferase system (PTS). *FEBS Lett* **504**: 104-111.

Singh, D., Fairlamb, M.S., Harrison, K.S., Weeramange, C., Meinhardt, S., Tungtur, S., Rau, B.F., Hefty, P.S., Fenton, A.W., and Swint-Kruse, L. (2017) Protein-protein interactions with fructose-1-kinase alter function of the central *Escherichia coli* transcription regulator, Cra. *bioRxiv*: 201277.

Swint-Kruse, L., and Matthews, K.S. (2009) Allostery in the LacI/GalR family: variations on a theme. *Curr Opin Microbiol* **12**: 129-137.

Tupin, A., Gualtieri, M., Leonetti, J.P., and Brodolin, K. (2010) The transcription inhibitor lipiarmycin blocks DNA fitting into the RNA polymerase catalytic site. *EMBO J* **29**: 2527-2537.

Ulrich, L.E., Koonin, E.V., and Zhulin, I.B. (2005) One-component systems dominate signal transduction in prokaryotes. *Trends Microbiol* **13**: 52-56.

Weickert, M.J., and Adhya, S. (1992) A family of bacterial regulators homologous to Gal and Lac repressors. *J Biol Chem* **267**: 15869-15874.

Yamada, M., and Saier, M.H., Jr. (1987) Glucitol-specific enzymes of the phosphotransferase system in *Escherichia coli*. Nucleotide sequence of the *gut* operon. *J Biol Chem* **262**: 5455-5463.

국문 초록

대부분의 박테리아 종에서, 과당 흡수는 과당-특이적 phosphoenolpyruvate: carbohydrate phosphotransferase system (PTS^{Fru})에 의해 매개된다. PTS^{Fru}는 과당 수송을 담당하는 막 단백질 인 FruA와 PEP에서 FruA로 인산기를 전달하는 FruB로 구성되며, 최종적으로 막을 통해 수송된 과당을 동시에 인산화한다. 대부분의 PTS 당은 6번째 탄소 위치에서 인산화되는 반면, 과당은 1번째 탄소 위치에서 인산화된다. Fructose 1-phosphate (F1P)는 1-phosphofructokinase (FruK)에 의해 fructose 1,6 bis-phosphate (FBP)로 전환된다. 대장균과 *Pseudomonas putida* 그리고 비브리오 콜레라를 포함하는 감마 프로테오박테리아에 속하는 박테리아는, FruA, FruB 및 FruK가 단일 오페론 (*fruBKA*)에 코딩되어있다. 대장균 및 *P. putida*와 같이 *fruBKA* 오페론을 보유한 대부분의 박테리아에서, *fruBKA* 오페론의 전사는 Fructose repressor (FruR)에 의해 음성 조절되며, 이는 전사개시시점 (TSS) 하류에 위치한 작용자에 결합함으로써 이뤄진다. F1P는 이 오페론 의 전사 개시 유도자이다. 그러나, 이 연구는 비브리오 콜레라균에있는 *fruBKA* 오페론의 FruR에 의한 전사 조절이 대장균 및 *P. putida*의 것과는 완전히 상이하고 더 정교하다는 것을 밝혀냈다. 비브리오 콜레라에서, FruR은 *fruBKA* 오페론의 전사 및 과당에서의 성장에 필수적이다. FruR은 FruR 자체를 코딩하는 유전자와 *fruBKA* 오페론 사이의 유전자 간 영역에 위치한 3 개의 작용자에 직접 결합한다. 이들 작용자 중에서, *fruBKA* 오페론의 TSS에서 20.5

bp 위쪽에 위치한 작용기는 *fruBKA* 전사의 활성화 및 과당에서의 비브리오 콜레라의 성장에 필수적이지만, 다른 두 작용기들은 그렇지 않다. 또한, FruR에 의한 전사 활성화는 세포 내 F1P를 필요로 한다. F1P 인식에 결함이있는 FruR 돌연변이체의 발현은 과당에서 *fruR* 결손 균주의 성장 결함을 회복 할 수 없었다. F1P는 작용기에 대한 FruR의 결합 특성을 변화시켜 RNA 중합체가 *fruBKA* 오페론의 전사를 활성화시킬 수있게한다. 이 연구에서는 비브리오 콜레라에서 FruR에 의한 비정규적인 *fruBKA* 오페론의 전사조절방식을 제시하고 있다

주요어:
과당대사; 과당특이적 PTS; FruR; F1P; 전사조절; 비브리오 콜레라

학번: 2013-20310